Wearable Inertial Sensors and Range of Motion Metrics in Physical Therapy Remote Support

University of Oulu
Department of Information Processing Science
Master's Thesis
Andrew Russell
03.12.2019

Abstract

The practice of physiotherapy diagnoses patient ailments which are often treated by the daily repetition of prescribed physiotherapeutic exercise. The effectiveness of the exercise regime is dependent on regular daily repetition of the regime and the correct execution of the prescribed exercises. Patients often have issues learning unfamiliar exercises and performing the exercise with good technique.

This design science research study examines a back squat classifier design to appraise patient exercise regime away from the physiotherapy practice. The scope of the exercise appraisal is limited to one exercise, the back squat. Kinematic data captured with commercial inertial sensors is presented to a small group of physiotherapists to illustrate the potential of the technology to measure range of motion (ROM) for back squat appraisal. Opinions are considered from two fields of physiotherapy, general musculoskeletal and post-operative rehabilitation. While the exercise classifier is considered not suitable for post-operative rehabilitation, the opinions expressed for use in general musculoskeletal physiotherapy are positive

Kinematic data captured with gyroscope sensors in the sagittal plane is analysed with Matlab to develop a method for back squat exercise recognition and appraisal. The artefact, a back squat classifier with appraisal features is constructed from Matlab scripts which are proven to be effective with kinematic data from a novice athlete.

Keywords
Physiotherapeutic exercise, back squat, wearable technology, e-health, smartwatch, kinematic, accelerometer, gyroscope, FFT

Supervisor
University Lecturer, Pasi Karppinen

Dedicated to Johanna, Torbjørn and Ukko.

Foreword

I would like to thank my thesis supervisor Pasi Karpinnen, University Lecturer, for his continued guidance and patience through the many twists and turns taken during my journey to write this thesis. I would also like to thank Professor Harri Oinas-kukkonen and Dr. Piiastiina Tikka of the OASIS research group, especially their enthusiasm for the theme of this thesis.

My gratitude is sincerely expressed to the students of physiotherapy and the practicing physiotherapists who generously gave their time and considered opinions to this study.

Detailed technical issues at times required assistance, and I would like to thank those who helped resolve these issues. Professor Markku Juntti, for questioning my methods for calculating derivatives. His expertise in digital signal processing proved to be essential. Mehdi Safarpour, Doctoral Student, for taking the time to explain the configuration of Fast Fourier Transforms and digital filters in Matlab. To my friend Florian Wolling for making great efforts to explain to me on more than one occasion, the Fourier series and transform.

Lastly, and most of all, I would like to pay tribute to my late grandfather, Alfred “Alf” Bates who worked night shifts as an engineer’s miller at Nottingham Royal Ordnance Factory (ROF) during the Blitz. He once said that the bombing was so close some nights that he imagined that he would never walk out of the factory. Suspecting he was being watched when he walked home past the house of a German lady, which had a telephone, he took the long route home, and for a while the air attacks ceased. He was quick to recognise his enemies. His financial contribution gave the means to write my master’s thesis while raising a young family. Thank you Grandad.

Andrew Russell

Oulu, November 11, 2019

Contents

List of Figures

List of Tables

Abbreviations

2D	Two Dimensions
3D	Three Dimensions (Tri-axial)
5G	Fifth Generation (mobile networks)
ACL	Anterior Cruciate Ligament
A/D	Analogue to Digital
BDM	Backwards Difference Method
BLE	Bluetooth Low Energy (wireless)
DC	Direct Current
DCM	Direction Cosine Matrix
DFT	Discrete Fourier Transform
DOA	Direction Of Arrival
DSP	Digital Signal Processor
DSR	Design Science Research
EMG	Electromyography
FCDM	First Central Difference Method
FEMO	Free-weight Exercise Monitoring
FFT	Fast Fourier Transform
FIR	Finite Impulse Response
HMM	Hidden Markov Method
HPA	Human Physical Activity
Hz	Hertz
IMMU	Inertial Magnetic Measurement Unit
IMU	Inertial Measurement Unit
KPF	Knitted Piezo-resistive Fabric
MEMS	Microelectromechanical Systems

NSCA	National Strength and Conditioning Association
OASIS	Oulu Advanced Research on Service and Information Systems
OMT	Orthopaedic Manual Therapist
OoS	Object of Study
PA	Physical Activity
PATD	Physical Activity Type Detection
PPG	Photoplethysmogram
PS	Performance Status
RFID	Radio Frequency Identification
ROF	Royal Ordnance Factory
ROM	Range Of Motion
STA	Soft Tissue Artefact
TAR	Technical Action Research
TEP	Total Endoprosthesis
TIFF	Tagged Image File Format

1. Introduction

Mobile and network technologies have become pervasive in recent years. A systematic review of wearable sensors in sport by Adesida et al. (2019), listed seven commercial wearable inertial systems used in the monitoring and coaching of sportsmen and women in athletics and eight other Olympic sports. Interconnectivity between smart devices is taken for granted, and the uses of such devices is ever expanding. Mobile technology has found its way into the field of physiotherapy, with companies such as Physiofile Oy offering an extensive video library for online physiotherapeutic exercises for remote rehabilitation and independent training (Physiofile, 2019). The company Physiotools Oy, has developed software enabling physiotherapists to create individual exercise regimes and send them directly to customers' computer, tablet or smartphone. Their subscription website allows the physiotherapist to select physiotherapeutic exercises from a menu which guides the physiotherapist through the affected area of anatomy and muscle sets (Physiotools, 2019). Once the physiotherapist has created the appropriate exercise regime, the physiotherapeutic exercise regime may be sent to the patient via email.

Having successfully prescribed a patient with a well targeted and considered physiotherapeutic exercise regime, physiotherapists must then rely on the honesty of their patient when reporting the times that the regime was executed between visits to the practice premises. Failure to continue the treatment away from the clinic is something that patients are reluctant to report. Validating patient's claims that exercises have been performed daily or as prescribed, is something of a difficult issue. The Physiotherapist may have prescribed an effective exercise regime with high efficacy, but if the patient does not perform the exercises as regularly as prescribed, the expected results will not be achieved in the anticipated timeframe. Patient adherence to rehabilitation programmes, particularly home exercises programmes is frequently low, and barriers to adherence have previously been identified within the literature (Picha & Howell, 2018). The effectiveness of tele-rehabilitation and remote patient monitoring on regime adherence had positive results suggesting further investigation into long term patient management (Peterson, 2018). How accurately or how well the patient executes the exercise is another factor that must be considered when assessing the recovery benefit of the exercise. If performed correctly the squat can enhance stability and be effective in developing hip, knee and ankle musculature through the activation of quadriceps, hamstrings and gastrocnemius (Escamilla, 2001).

The validation of patient exercises is an area of physiotherapy that has already been considered. A mobile application that records patient input after performing exercises is currently in use. PT-Momentum, a mobile application developed by Physiotools, which works in conjunction with the Physiotools web site, prompts the patient to confirm the physiotherapeutic exercises performed each day. Patient trust is relied on to enter only honest data. Patients not performing their prescribed physiotherapeutic exercises at home between control visits to the clinic, may result in longer treatment times. Consequently, the therapy is not time and cost effective, since time is lost in the treatment process and rehabilitation time is lengthened. By appraising patients who regularly perform physiotherapeutic exercises at home, the aim is for the therapy to become more effective, and overall health care costs for society are reduced. This study

aims to find viable methods for processing kinematic data from wearable inertial sensors to recognise and appraise back squat exercise. The aim of the methods sought is to form the basis of an exercise classifier applied to a wearable inertial sensors system for patients following a physical therapy regime.

2. Research problem and research methods

The overall aim of this study to construct a new artefact, a sequence of Matlab scripts that are proven methods, able to recognise and appraise back squat exercise through the processing of kinematic data from wearable inertial sensors. The classifier methods could then be used in a further study to develop a system to aid patients in performing physiotherapeutic exercise in their home environment. The term aid in this context refers to patients who for whatever reason do not perform their physical therapy exercise regime without the presence of their physiotherapist. The objective is to provide real-time feedback on the quality of the exercise being performed. The motivation for the study is the premise that patients who would ordinarily fail to exercise without the presence of their physiotherapist, would be motivated by a system that monitors their exercise, giving real-time appraisal and encouragement. The real-time monitoring and appraisal of exercise, promotes correct technique, engaging the desired muscles sets, thereby speeding rehabilitation.

The scope of the research is too wide to be studied in entirety. To reduce the scope, the study focus is limited to a single commonly prescribed physiotherapeutic exercise, namely back squats. The choice of exercise is based partly the author's own experience in the gym, where back squats were found to be quite technical and required coaching in order to be performed with any degree of proficiency. Back squats are commonly prescribed for musculoskeletal injuries because of its similarity and applicability to both activities of daily living and many athletic movements. It is a multipoint movement that requires many muscle groups to function together (Cotter et al., 2013). Over two hundred muscles are activated during squat exercise (Schoenfeld, 2008). In rehabilitation they are often prescribed including for example following anterior cruciate ligament (ACL) reconstruction (Horschig et al., 2014).

2.1 Research problem

To understand how wearable inertial sensors could be applied to monitoring and coaching patients performing back squats as part of their physical therapy. The following research question needs be answered.

1. What are the viable methods for processing kinematic data from wearable inertial sensors to recognise back squat exercise and provide metrics for a system that gives exercise technique appraisal?

This study begins by researching the current inertial systems used by the professions of medicine and physiotherapy to monitor and classify patient physical activity. The study continues to examine wearable inertial human motion capture systems generally available to the other professions. The first research question is answered in the background literature section. The second research question is answered by literature analysis and the application of wearable inertial sensors manufactured by Xsens B.V., generously loaned by the University of Oulu Medical School. The Xsens MTx wearables are utilized in a laboratory experiment for the generation of ideal data for back squats, from the sacrum, thigh and shank. The results of the experiment to generate

ideal kinematic data are used to propose a system which is discussed with practising physiotherapists. The ideal kinematic data is analysed further by several methods to achieve quantitative measures of back squat exercise that are suitable for an exercise system classifier.

2.2 Research methods

The research conducted in this study is constructive and evaluative by nature. The ideas of constructive research are eloquently described by the multi-methodological to information system research (Figure 1) developed by Nunamaker, Chen, and Purdin (1990). The multi-methodological approach consists of four research strategies: theory building, experimentation, observation and system development.

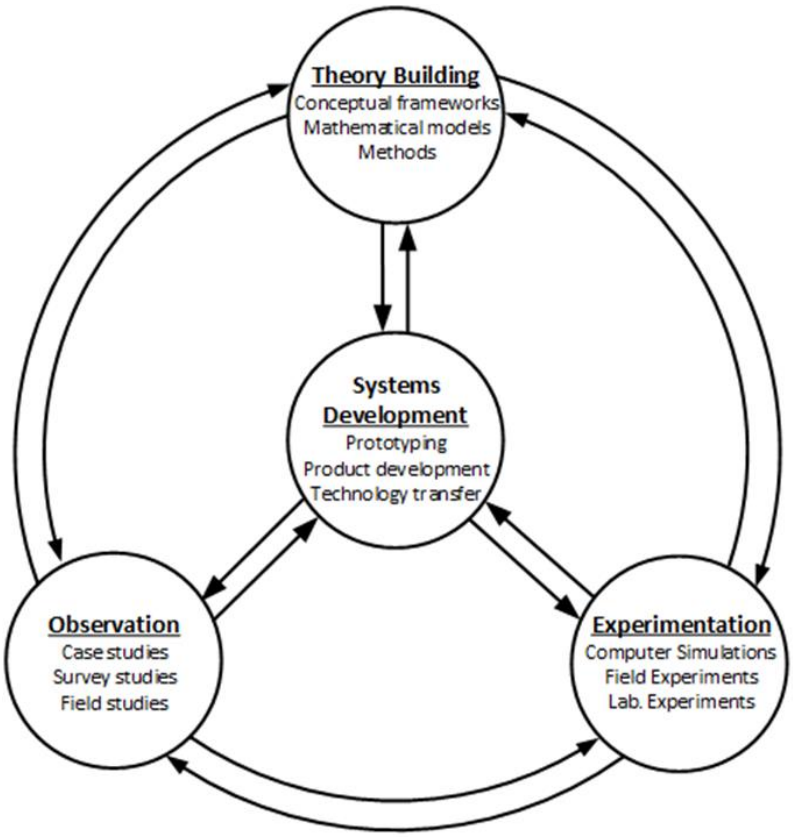

Figure 1. A methodological approach to Information System Research (Nunamaker, Chen, and Purdin, 1990).

The theory building construction is based on a thorough understanding of the field under study. The approach taken by Nunamaker et al., (1990), was one of achieving understanding through observation activities. In this thesis, instead of observations, a background literature analysis is conducted to familiarize with the current technology and deployment of wearable inertial sensors in relation to human motion capture and analysis. Literature analysis is considered suitable, because it provides a broader understanding of human motion capture than attempting to cover all of the techniques used with a case related field study.

The background study also serves to identify a subset of physiotherapeutic exercise that is suited to monitoring by wearable inertial sensors with previous research to identify the metrics that define the quality of the physiotherapeutic exercise performed. From the metrics of exercise analysis, a theoretical system design utilizing current wearable inertial sensors is proposed.

The theory building starts with a background review of literature and the analysis of the existing systems for biomechanical analysis and e-health systems utilized by practicing physiotherapists. The aim of the system is to provide patients exercising at home with encouragement and guidance or coaching based on the data provided by the wearable inertial sensors. The initial system design process is evaluated by a presentation of the proposed system followed by interviews with practicing physiotherapists.

The data capture by inertial sensors is tested in a laboratory experiment with wearable inertial sensors manufactured by Xsens. The data is acquired from an experienced physiotherapist and researcher of biomechanics, performing a sequence of six back squats while wearing the Xsens MTx sensors on the sacrum, thigh and shank. The aim of the experiment is to validate if the data is appropriate for evaluating the quality of physiotherapeutic exercise being performed. The captured data is used to research suitable techniques for signal processing and data analysis. Moreover, the laboratory experiment provides the means to conclude if the technical specifications of the Xsens MTx wearables, the resolution and sampling rate are adequate for physiotherapeutic exercise analysis. The data is analyzed within the Matlab environment using Fast Fourier Transform (FFT).

2.3 Design science research

Design science research (DSR) is a research framework that is utilized in the development of a new artefact. The artefact may be a new information system in its entirety, or as is more common, and in the case of this study a new method or process to be used by an existing information system. DSR consists of three cycles of activities, the relevance cycle, the central design cycle, and the rigor cycle (Hevner, 2007). In the relevance cycle defines the requirements from the contextual environment. The rigor cycle provides grounding theories and methods and adds new knowledge generated by the research to the knowledge database. The central design cycle conducts construction and evaluation for design artefacts and processes. The DSR framework is illustrated in the figure below by Hevner et al., (2004), which illustrates the iterative nature of the framework, and the relevance and rigor tests conduct during the research cycle.

The fundamental principle of design-science research is that knowledge and understanding of a design problem the solution are acquired in the building and application of an artefact. From these fundamental principles, the seven guidelines for DSR are derived (Hevner et al., 2004).

Guideline 1: Design as an artifact. The result of design-science research in IS, by definition, is a purposeful IT artefact created to address an important organizational problem, which is described effectively, enabling implementation and application in an appropriate domain. Artefacts are seldom complete information systems, rather innovations that define ideas, practices, and products through which the analysis, design, implementation and use of information systems can be effectively and efficiently accomplished (Denning 1997; Tsichritzis 1998).

Guideline 2: Problem relevance. The research objectives in IS are to gain knowledge and understanding that enable the development and implementation of solutions to previously unsolved business problems. Behavioral science takes an approach that develops theories to explain or predict phenomena, whereas DSR takes a different approach, that of the construction of an artefact specifically aimed at changing the phenomena that occur. The definition of a problem is defined as the differences between the current state and a goal state. Therefore, problem solving can be defined as a search process using actions to reduce or eliminate the differences (Simon 1996). This implies that the environment imposes goal criteria as well as constraints upon a system. In a business environment, problem solving may have goals which involve reducing costs and increasing revenues. A study by Simon in 1996 states, "solving a problem simply means representing it so as to make the solution transparent."

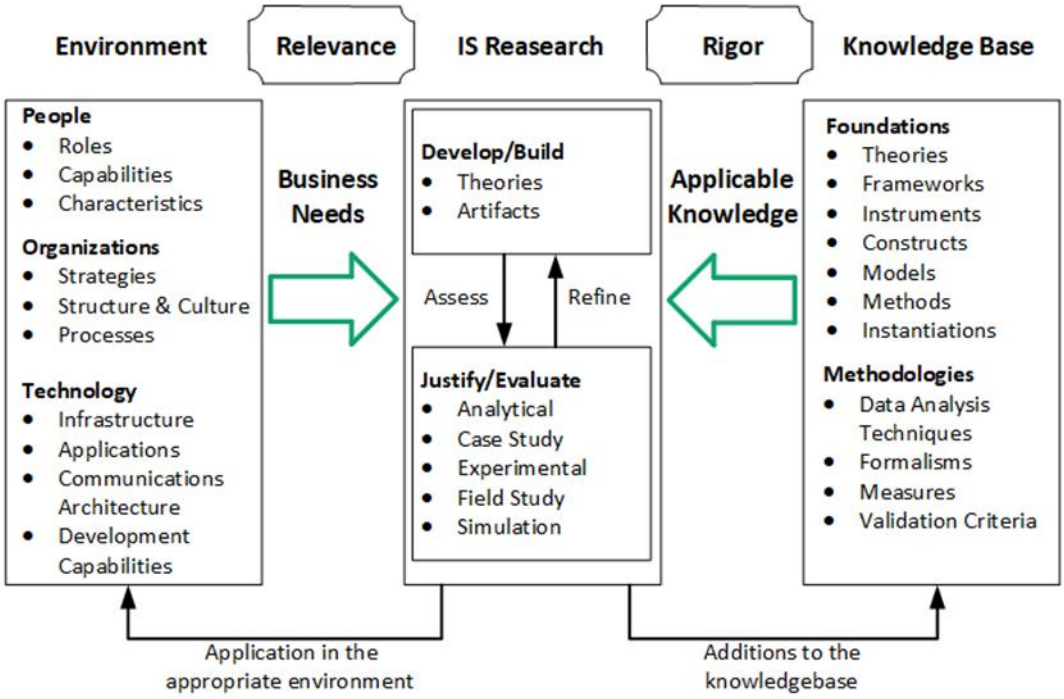

Figure 2. Information Systems Design Research Framework (Hevner et al., 2004).

Guideline 3: Design evaluation. In behavioral science theory justification is required, and this is also true of DSR artefacts. In IT evaluation of a designed artifact requires the definition of appropriate metrics, and possibly the collection and analysis of appropriate data. Due to the inherently iterative and incremental nature of design, the evaluation phase provides essential feedback to the construction phases. The feedback is essential for the quality of the design process, and the quality of the design product under development.

Design evaluation is performed by one of the five methods available in the knowledge base, observational, analytical, experimental, testing and descriptive. In this study analytical evaluation is a dynamic analysis with wearable sensors collecting data during physical exercise. Experimental analysis is conducted with wearable IMMU sensors in a gym environment. Descriptive analysis is conducted with informed argument based on interviews with practicing physiotherapists in the fields of musculoskeletal, and post-operative rehabilitation.

Guideline 4: Research Contributions. The deign-science research must provide clear contributions in the areas of the design artefact, and design construction or design evaluation knowledge. The assessment of an artifact must answer the question “what are the new and interesting contributions?”

Guideline 5: Research Rigor. Addresses the manner in which the research was conducted, in both the construction and evaluation of the artefact. In both design-science and behavioral-science research, rigor is derived from the effective use of the knowledge base, theory and research methodologies. The research rigor assess’ the researcher’s ability to select appropriate techniques to construct a theory or artefact.

Guideline 6: Design as a Search Process. Design science is an iterative process, searching for the best or optimal solution to reach a desired goal within the context of the operating environment. A problem may be satisfied by a set of several design solutions. The research challenge being a search to identify a design as the optimal solution for the specific end use conditions. Using heuristics to find a good design solution raises the question of how goodness is measured. It should be established that the artefact does work, even if we are unable to explain why. Researchers are then able to utilize the new artefact in additional research to fully explain the resultant phenomena.

Guideline 7: Communication of Research. The artefact must be described in sufficient detail to enable the described artefact to be constructed. Also, it is important that the processes by which the artefact was constructed and evaluated are described such that the research is repeatable, building the knowledge base for further research extensions (Hevner et al. 2004.)

From literature (Wieringa, 2014), DSR is the design and investigation of artefacts in context, where an artefact is designed to interact with a problem to achieve an improvement to the problem in that context. The design of an artefact may be achieved in one of two directions and is referred to as the direction of arrival (DOA). In the first DOA an artefact is designed to improve a problem when is then studied in context. In the opposite direction, new knowledge is gained from the artefact in context, resulting in new design issues which are applied to a new artefact design iteration.

Research goals in DSR are dependent on the type of study undertaken. A problem investigation has the research goal of investigating an improvement before an artefact is designed, and where no requirements for the artefact have been defined. An implementation evaluation has the goal of evaluation of the implementation of a treatment after it has been applied (Wieringa, 2014). In this study interviews were conducted with physiotherapists to gain the requirements of the system before the implementation of a back squat exercise classifier. The object of study (OoS) being the back squat exercise classifier, composed of Matlab scripts, that processed kinematic data from back squat exercise. From the interview responses, laboratory experiments were conducted with test data that was considered appropriate for the context of the problems experienced by general musculoskeletal physiotherapists.

A stakeholder of a problem is a person, group of persons or institution affected by treating the problem (Wieringa, 2014). A negative stakeholder is someone who would be made worse off when the artefact is introduced to the problem context. In this study for example, post-operative physiotherapists could be considered negative stakeholders if the wearable system is able to accurately measure knee valgus. Replacing their

expertise, being able to assess gait by observation with a wearable system, may imply to some that their expertise is no longer appreciated.

3. Background

3.1 System architecture for e-health in medicine

Gresham et al., (2018) conducted a prospective, single-center, single-cohort trial to evaluate the use of commercially available Fitbit activity monitors for the measurement of daily activity in advanced cancer patients. The activity monitors measured heartrate and steps taken. The step count being sensed with accelerometer sensors. The study assessed if activity monitors would be of use in the evaluation of patient Performance Status (PS) and survival in advanced cancer patients. The objective evaluation of patient PS is challenging since patients spend most of their time outside of the clinic and undergo dynamic changes throughout the treatment cycle. Real time objective data allowed for a more accurate assessment of PS.

Statistical methods used included multivariable regression models to evaluate the associations between performance status and wearable activity monitor metrics. The activity metrics were based on an estimated 5000 steps per da. The evaluation confirmed activity data could supplement clinical evaluation of performance status. The activity data was also able to suggest a trend for the prediction of clinically relevant events, 30 day morbidity, and 6 month survival. Correlations were also observed between activity monitor metrics and physical functioning, pain, fatigue and emotional distress (Gresham et al. 2018.)

3.2 Sensor systems

The study aims to use wearable sensors to capture kinematic data of human body motion during exercise. Kinematic data being the observed forces experienced by body segments, not the forces exerted by muscles, or the resulting stresses experienced on the musculoskeletal system. The three main sensors types used are accelerometer, gyroscope, and magnetometer. Many smartphones and watches use one or more of these sensors, and it is important to understand the different variations which effect the usefulness of each variation for the task assigned. Many motion capture systems use sensors systems that combine several types of sensor in software, to enhance the accuracy and reliability of the kinematic data captured.

A study conducted by Shen et al. (2018) described the design and implementation of a system utilized commercially available smartwatches to accurately track both cardio and weight-lifting workouts automatically, with above ninety percent accuracy. The smartwatch selected utilized a photoplethysmogram (PPG) heartrate sensor, but more importantly featured accelerometers and gyroscope sensors. The data from the accelerometers and gyroscope sensors were combined in software to create a gravity sensor. The gravity sensor is a composite sensor that is described in the online technical support pages of Android smartwatches. In the study, the Moto 360 smart watch was effectively used. It was able to detect fifteen different weight-lifting machine and free weight exercises by identifying the unique 3 axis gravity sensor data patterns.

Devices with gyroscopes and accelerometers are considered in this study for a system to give persuasive feedback to patients during physiotherapeutic exercise. While sensor design is beyond the scope of this study, sensors that are able to capture specific types of body motion are of particular interest. Smartwatches are able to detect wrist orientations and torso movements, whereas smartphones carried in pockets are only able to detect body postures (Shen et al., 2016).

The accurate measurement of Human Physical Activity (HPA) and the identification and quantification of different types of physical activity (PA) is one of the challenges of PA research in the area of cardiovascular health (McCarthy and Grey 2015). Among the existing portable sensors used in smartwatches and smartphones, accelerometers have been the subject of most studies (Shoaib et al., 2014). Since accelerometers may be produced in miniature form and are light weight, they have become common place in mobile phones and wearable PA systems. Accelerometers record information on acceleration which may be processed to reveal type of movement and activity performed by users. Many different methods exist for collecting and analyzing data from PA systems, prompting in a review of the literature in PA monitoring with a focus on PA Type Detection (PATD) in real life situations using accelerometer measurements (Allahbakhshi et al., 2019).

Accelerometers are manufactured in three different types, uni-axial (1D), dual-axial (2D), and three-axial (3D). Multi-axial accelerometers give data in multiple dimensions, improving the accuracy of PATD models. More distinct features are able to be extracted from 3D accelerometers than by 1D or 2D accelerometers since they provide data in three orthogonal dimensions. With real-life data collection, the number and placement of accelerometers is challenging, as shown by a study by De Vries et al., (2011) found that accelerometers were required to be placed on both the hip and ankle when detecting postures and activities such as sitting, standing, stair ambulation, and cycling. It concluded that a single hip-worn accelerometer alone is insufficient for accurately detecting activities. This is supported in a study by Gyllensten and Bonomi (2011) which used only a single waist-mounted 3D accelerometer with laboratory trained algorithms, the results of which proved problematic in the classification of real-life activity.

Three dimensional accelerometers have their limitations, for example with wrist worn smartwatches the amplitude of signals generated increase with the arm length of the user. Thus, creating a model that accurately detects physical activity type becomes problematic since signal size varies with user size as well as activity type. To overcome this problem in recent years other sensors such as the gyroscope and magnetometer have been combined with accelerometers to build inertial magnetic measurement units (IMMU) which improve the performance of activity recognition (Shoaib et al., 2014).

3.3 Human body motion capture suites

A study by Rotenburg et al., (2009), examined the Xsens MVN human body motion suite (Figure 3) which uses 17 proprietary Xsens MTx IMMUs to capture body motion. The MVN system has found use not only in analysis of human ambulation analysis for rehabilitation, but also for character choreography in the computing gaming industry. The fusion of accelerometer, and gyroscope data, gives 6 degrees of freedom in orientation measurement. Human joints allow some laxity in all directions thus human movement modelling is not possible with pure hinge joints, and ball and socket joints, thus 3 degrees of movement is insufficient. The inertial magnetic measurement units

(IMMUs) additionally utilize 3D magnetometers to gain earth frame heading information. Compensation for drift errors in gyroscopes is maintained by integrating accelerometer rate data. Magnetometers provide a reference in the horizontal plane using the geomagnetic field to define heading. The magnetic sensing algorithm, in the latest MTi sensors from Xsens, contain filtering mechanisms provided by a magnetic field mapper to counter-act disturbances in the geomagnetic field caused by ferrous metals in close proximity. The earlier MTx IMMUs used in this study are not immune to ferromagnetic disturbances (Rotenburg et al., 2009.)

Figure 3. Xsens MVN wireless motion capture suite (Rotenburg et al., 2009)

The application developed by Xsens to visualize data collected by the MVN motion capture suite is animated in the MVN motion application. Human motion capture (mocap) data may be exported to other mocap systems including 3ds Max, XSI, and MotionBuilder.

Figure 4. Xsens MVN Studio (Rotenburg, Luinge and Slycke 2009)

Data capture from the MVN motion capture suite is animated in the MVN Studio application. Human motion capture (MOCAP) data may be exported to other MOCAP systems including 3ds Max, XSI, and MotionBuilder (Figure 4).

A study by Mourcou et al. (2015) evaluated the accuracy of the MTx sensor as compared to smart phone inertial sensors under clinical conditions, where motion was controlled with a robot arm. Data was processed with three different filters, the manufacturers', Madgwick and Mahony. The results listed MTx roll and pitch RMS errors were less than 0.3 degrees. The smartphone inertial sensors gave good results of a similar order of error as the MTx sensors, the study conclude there were no significant differences between the three smartphones selected and the MTx sensors.

3.4 Earth frame orientation

Unlike motion tracking systems that are based on computer vision, inertial sensors have no fixed orientation. Cameras used in computer vision systems such as Vicon, are placed in a stationary fixed position at a known point and heading. Wearable sensors conversely, do not maintain a fixed position and heading since they are attached to body segments of a person who moves.

For a human motion capture system that utilizes inertial measurement units (IMUs) the motion capture system must be informed of the orientation of each IMU manually. Once the orientation of the sensors at the start of the motion capture sequences is set, subsequent samples from the IMUs give incremental changes to the starting orientation. Thus, a plot of linear motion is the result of the cumulative summation of accelerometer samples. A plot of rotational movement is the cumulative summation of the changes in IMU angle, but for these changes to have orientation in the real world, they must be relative to a known fixed reference point.

An inertial magnetic measurement unit (IMMU) contains a tri-axial magnetometer, as well as tri-axial accelerometers and tri-axial gyroscopes. At rest the accelerometers will experience the earth's gravitational acceleration, 'g' which is approximately 9.8 meters per second per second in the downwards direction or 'z' axis. If the z axis accelerometer is not facing directly down, then the earth's gravitational acceleration will be sensed in two or more axis, the combined vector sum of which will equal one 'g'. With a tri-axial accelerometer it is possible to calculate the downwards orientation of the z axis. Since the IMMU has a tri-axial magnetometer, the orientation of the earth's magnetic north pole is obtained. Internal to the IMMU, the magnetometer and accelerometer are aligned. This physical alignment inside the IMMU allows orientation heading to be added accelerometer sampled data. The sensing and combination of the earth's gravitational and magnetic field is referred to as earth-frame or earth-fixed frame orientation (Zhou and Hu, 2009) (Sabatini, 2011).

The presence of geomagnetic distortions is common in everyday life, for example inside a car, or inside a gym with iron barbells and the steel frames of training machines. In order to obtain accurate orientation estimates, not only must the magnetometer and inertial sensors be accurately aligned, but also be calibrated for sensor errors and magnetic distortions. Algorithms have been developed to overcome any static magnetic distortions. Geomagnetic data collection is assumed to be collected by a sensor rotating in all possible orientations, implying that the magnetometer data lies on a sphere. The presence of magnetic distortions and or magnetometer sensing errors, will instead cause the magnetometer data to lie on an ellipsoid. To compensate for the sensor calibration errors and static magnetic disturbance errors, require the ellipsoidal magnetic data to be

mapped to a sphere, the radius of which is equal to the local magnetic field (Kok et al.,2012.)

3.5 Euler angles and quaternions

Gyroscopes used for navigation systems are usually suspended in a gimbal mechanism to allow the gyroscope to maintain its position while the supporting chassis moves freely relative to it. To allow movement in 3 axes of rotation, a set of three gimbals are mounted together to allow three degrees of motion in the x, y and z axis, otherwise referred to as roll, pitch and yaw. When one gimbal rotates a full ninety degrees, two gimbals rotate around the same axis, and one degree of freedom is lost, a state known as gimbal lock. A work around is to add a fourth gimbal, which adds a forth rotational axis, but this still requires to be actively orientated ninety degrees out of alignment with the inner most axis. Else at least maintain a large maintain a larger angular difference between the roll and yaw gimbal axis. This is because as a gimbal approaches the same axis as another gimbal, the force to move the gimbal increases rapidly until at ninety degrees the force to gimbal rotation becomes infinite. To avoid gimbal lock, modern navigation systems mount inertial sensors directly to the chassis of the vehicle, this type of system is a strap down navigation system. The strap down system uses integrated digital sensors to sense rotation and acceleration, and quaternion mathematical methods to derive orientation and velocity.

All possible orientations are able to be described by composing three rotations about the axes of a coordinate system. Leonhard Euler, an eighteenth century, Swiss mathematician, introduced Euler angles to describe the orientation of a body by rotations about three axis' of the coordinate system, performed in a particular sequence. Euler proved that the sequence of the three rotations of the body is non communitive. Three parameters are always required to describe orientations in a 3-dimensional Euclidian space. Euler's rotation theorem states that in 3-dimensinal space, the displacement of a rigid body, such that a point on the rigid body remains fixed, is equivalent to a single rotation about an axis that runs through the fixed point. This also proves that the composition of two rotations is also a rotation. The set of rotation has group structure, known as a rotation group (Euler, 1776).

The Euler angle sets are the classical minimum parameter attitude, therefore they have the problem of being singular at either

$$\theta_2 = 0, \pi \ or \ \theta_2 = \pm\frac{\pi}{2} \tag{1}$$

Despite their issues with mathematical singularity when pitch approaches plus or minus ninety degrees, Euler angles are easy to visualize, which makes them popular for many attitude (pitch) determination applications. For the asymmetric Euler angle sets $\theta_2 = \pm\pi/2$ results in geometric singularity. For the symmetric Euler angle sets the geometric singularity occurs when the angle theta two equals zero or plus or minus pi radians, as described in Equation (1) (Singla et al., 2004.)

Euler angles describe rotation of a body by means of three successive rotations in a particular sequence. Euler angles use roll, pitch and yaw, known as the Cardan or Tait-Bryan angles. This follows the aerospace convention of the z-axis, y-axis, x-axis sequence. Euler angles follow the aerospace convention. To convert from the global

reference co-ordinate system to sensor co-ordinate system the rotation matrix, also known as the Direction Cosine Matrix (DCM) is applied, which can also be expressed in terms of quaternions.

This study uses Xsens MTx IMMU sensors which describe 3D-orientation in terms of φ (phi) = yaw or heading, θ (theta) = pitch or elevation, ψ (psi) = roll or bank. Where φ = yaw, the rotation around the z-axis is defined as -180° to 180°, θ = pitch, the rotation around the y-axis, defined from -90° to 90°, ψ = roll, rotation around the x-axis is defined from -180° to 180°. By default, the local earth-fixed reference co-ordinate system used is defined as a right-handed Cartesian co-ordinate system with: x-axis positive when pointing magnetic north, y-axis positive according to right handed co-ordinates west, and z-axis positive when pointing up (Xsens Technologies, 2006).

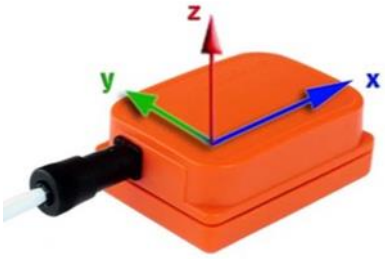

Figure 5. Xsens MTx sensor-fixed co-ordinate system (Xsens Technologies, 2006)

The Xsens MTx IMMU sensors provide rotation matrices to perform calculations on relative positions of the sensors 3D-orientation to the global reference co-ordinate system in terms of Euler angles (Pérez et al., 2010).

$$R = R_{\psi}^{Z}.R_{\theta}^{Y}.R_{\varphi}^{X} =$$

$$\begin{bmatrix} \cos\psi & -\sin\psi & 0 \\ \sin\psi & \cos\psi & 0 \\ 0 & 0 & 1 \end{bmatrix}.\begin{bmatrix} \cos\theta & 0 & \sin\theta \\ 0 & 1 & 0 \\ -\sin\theta & 0 & \cos\theta \end{bmatrix}.\begin{bmatrix} 1 & 0 & 0 \\ 0 & \cos\varphi & -\sin\varphi \\ 0 & \sin\varphi & \cos\varphi \end{bmatrix} \quad (2)$$

To avoid gimbal lock singularities, MTx IMMU sensors utilise quaternions as an efficient and non-singular alternative representation of their orientation. Quaternions can be interpreted as a rotation through an angle α about a unit vector n:

$$n = \left(\cos\left(\frac{\alpha}{2}\right), n.\sin\left(\frac{\alpha}{2}\right)\right) \quad (3)$$

Quaternions were first devised by William Rowan Hamilton, a 19th-century Irish mathematician. Using unit quaternions to represent the attitude of an object completely avoids the problem of gimbal lock (Diebel, 2006).

To obtain singularity free rotation matrices from quaternion representation, Equation (4) must be applied:

$$R = \begin{bmatrix} 2q_0^2 + 2q_1^2 - 1 & 2q_1q_2 - 2q_0q_3 & 2q_1q_3 + 2q_0q_2 \\ 2q_1q_2 + 2q_0q_3 & 2q_0^2 + 2q_2^2 - 1 & 2q_2q_3 - 2q_0q_1 \\ 2q_1q_3 - 2q_0q_2 & 2q_2q_3 + 2q_0q_1 & 2q_0^2 + 2q_3^2 - 1 \end{bmatrix} \quad (4)$$

Given Equation (2), sensor roll φ (phi), pitch θ (theta) and yaw ψ (psi), are obtained with the following formulae:

$$\varphi = roll = \tan^{-1}\left(R_{3,2}/R_{3,3}\right) \quad (5)$$

$$\theta = pitch = \sin^{-1}\left(R_{3,1}\right) \quad (6)$$

$$\psi = yaw = \tan^{-1}\left(R_{2,1}/R_{1,1}\right) \quad (7)$$

In Equations (5) and (7), the arctangent is the four-quadrant inverse tangent function (Pérez et al., 2010.)

3.6 Squat exercise kinematics

An assessment of the back squat by Myer et al. (2014) describes the fundamental movements and skills required to perform the back squat exercise while mitigating the risks of injury. First it is advised that the participant be fully proficient at the body weight squat before attempting externally loaded squats, since the exercise creates shear forces on the lower spine.

The starting posture is described a standing with feet flat on the floor, hip width apart, feet alignment parallel to 10 degrees turned out following the natural turn out of the leg. Weight is applied mid foot to aid balance. Knees and his are in a neutral extended

anatomical position, with the spine in a neutral upright position preserving the natural curves. The lumbar and cervical spine maintain their lordotic curve, the thoracic and sacral spine maintain kyphotic curves. The breath should in hail up to 80% and be held in eccentric phase (descent). The dowel is placed across the upper back on the trapezius muscle. At the start of the eccentric phase the hips, knees and ankles flex, continuing until the thigh is parallel or slightly lower to the ground. Thus, are often referred to as parallel squats. The pelvis tilts forwards and moves backwards to some extent to maintain balance. The back is kept close to vertical to keep shear forces to the lower back to a minimum. There is some forward tilt of the rigid back, the angle of which is close to that of the shank, sometimes described as the spine and tibia being parallel in the sagittal plane. The knees extend forwards past the toes in what is referred to as an unrestricted squat. The concentric phase (ascent), is achieved through the triple extension of the hips. The posterior torso muscles in particular the erector spinae, are engaged by isometric muscle action to support the posture throughout the entire squat movement.

A study of the back squat by Fry et al. (2003) examined the effects of keeping the shanks near vertical, and behind the toes during the entire squat sequence, referred to as a restricted squat. A vertical board placed in front of the toes to above knee height physically restricted knee movement forwards beyond the toes. The restriction on the knees results in knee torque becoming less than hip torque, arguably creating less stress on the knees. The increased hip torque creates a change in the center of gravity which is compensated for in a greater inclination forward of the torso. Except with experienced lifters who maintain balance with a more erect posture and a greater extensor dominant thigh torque. The study concludes that although restricted squats reduce the stresses on the knees, it is likely that forces are inappropriately transferred to the low back region.

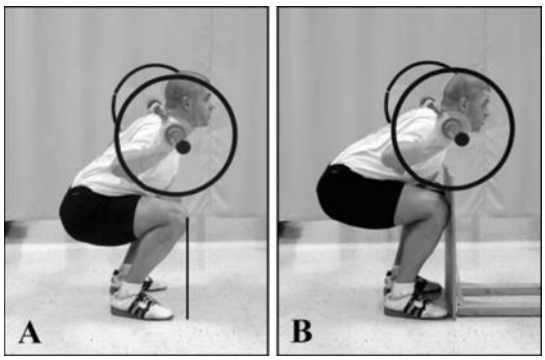

Figure 6. (A) Unrestricted squat, where the knees are able to move anteriorly as far as necessary. Note the line illustrating the amount of anterior displacement of the knees relative to the toes. (B) Restricted back squat, where a vertical board restricts anterior knee displacement (Fry, 2003).

A study of the comparison of angles and corresponding moments in knee and hip during restricted and unrestricted back squats by Lorenzetti et al. (2012) analyses measurements from ten female and ten male subjects. The results found that for restricted squats the maximum knee moments were 22.4% less than for unrestricted squats. The maximum hip moments for restricted squats were 6.9% higher than unrestricted squats. The maximum moment of knee being at the lowest point of squat at the knee flexion angle of approximately 83 degrees for restricted squats, and approximately 104 degrees for unrestricted squats. At the lowest point ankle flexion is 21.3 degrees for restricted and 31.5 degrees for unrestricted squats. Hip flexion was found to be similar, but slightly larger for unrestricted squats.

The study concluded that a compensatory mechanism in the upper body is required to execute restricted squats to maintain balance and simultaneously align shins vertically. The maintenance of a normal lordotic torso posture results in significant hip flexion during restricted squats. This movement is contrary to National Strength and Conditioning Association (NSCA) guidelines which specify that the torso should be close to vertical during the entire lift. It is interesting to note that in the study by Fry et al. (2003) there also NSCA guidelines which cite the need to keep the knees from moving forward past the toes or to keep the shank as vertical as possible when performing the exercise. Clearly there are different techniques utilised in performing back squats and the design of a system to appraise the position of knees relative to toes would require some form of musculoskeletal model to reference. The complexity of such a model deem it outside the scope of this study.

As the study of Lorenzetti et al. (2012) states, because weight overload or improper executions, squats are associated with one of the highest rates of injury at Swiss fitness centers, half of which involve the lower back. Correct back alignment is required form the outset since it is quotes as this is when the lower back experiences the most shear force. The study gives standard instructions which advise the athlete to lift the thorax to a neutral spinal position and to hold the tension in the core muscles throughout the squat, breathing out during the concentric phase.

With the description of a neutral spine somewhat difficult to comprehend for athletes new to the back squat, technique described in classical ballet may be found to be useful in achieving a neutral spine. From literature Warren (1989), the correct stance is achieved using the central muscles at the base of the ribcage, the dancer holds the ribs in and flat, thus, she (or he) is able to control the lower back and stabilise the vertical placement of the torso above the supporting leg(s). The correct posture is described as the chest to be maintained flat, thorax lifted up, ribs in, and muscles below the ribcage engaged in an upwards direction. When the ribs are inflated and thrust forward, the result is a swayed back. A swayed back results in increased kyphotic curve of the thoracic spine and increased lordotic curve of the lumbar region. This artificial placement of the torso is anatomically unhealthy and will prohibit freedom of movement (Warren, 1989.)

A study by Lorenzetti et al., (2018) examined in laboratory conditions back squat exercises performed by several groups varying from novice to highly experienced. Vicon optical marker-based motion capture cameras, and floor mounted force plates to measure kinematics, range of motion and kinetics. The motion capture Vicon system comprised of 29 cameras at a sampling frequency of 100 Hz. Kinetic data was captured with two Kistler forces plates, one under each foot, using a sampling frequency of 2000 Hz. The marker set consisted of 55 markers on the legs, pelvis, shoulder, and arms, with 22 on the back, and 2 attached to the wooden bar or barbell (Figure 7).

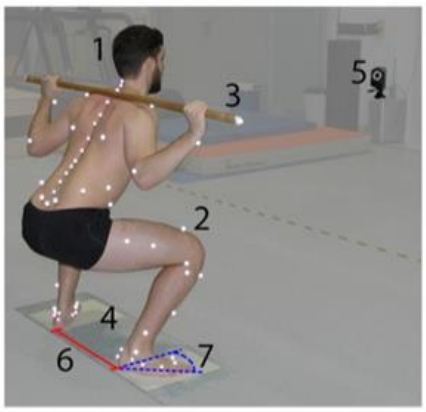

Figure 7. Back squat exercise measurements as stance and foot angle vary (Lorenzetti et al. 2018)

A single squat cycle consisted of participants starting from upright, moving downwards to the lowest point possible, and returning to the upright position. Instructions were given to all participants (Table 1) before performing back squats in the biomechanics laboratory.

Table 1. Standardised instructions for back squat performance. (Lorenzetti et al., 2018)

#	**Instructions**
1	Place the bar (barbell) on the trapezius muscle and hold it with a comfortable hand position.
2	Stand upright and place each foot on one of the given lines. Keep the heel and second toe aligned.
3	Keep your back straight throughout the movements.
4	Perform the squat at the same speed in the downward and upward movements.
5	Try to go as far downward as possible, at least bringing your thigh parallel to the floor.

In the study by Lorenzetti et al. (2018), the vertical velocities of the two barbell markers were tracked. Leg true alignment was defined as deviation from the knee joint centre, in the sagittal plane with standard deviation defined in percentage leg length. The alignment of each of each leg measured from the head of the second metatarsal, ankle joint centre, the hip joint centre. Leg misalignment, knee valgus and knee varus were measured. The participants performed squats with a range of stance widths and range of foot placement angles. The kinematics of average mean knee deviation from straight alignment was measured as a percentage of the participants' leg lengths. The results revealed values of standard deviation from true leg alignment were between -17% and 27% of participants' leg length, indicating valgus and varus positions. Significant differences in standard deviation were found between novice and experienced squatters, as well as factors of stance width and foot placement angle. It was found that wider stance gave a smaller standard deviation, a wider foot placement angle caused a larger standard deviation (Lorenzetti et al. 2018.)

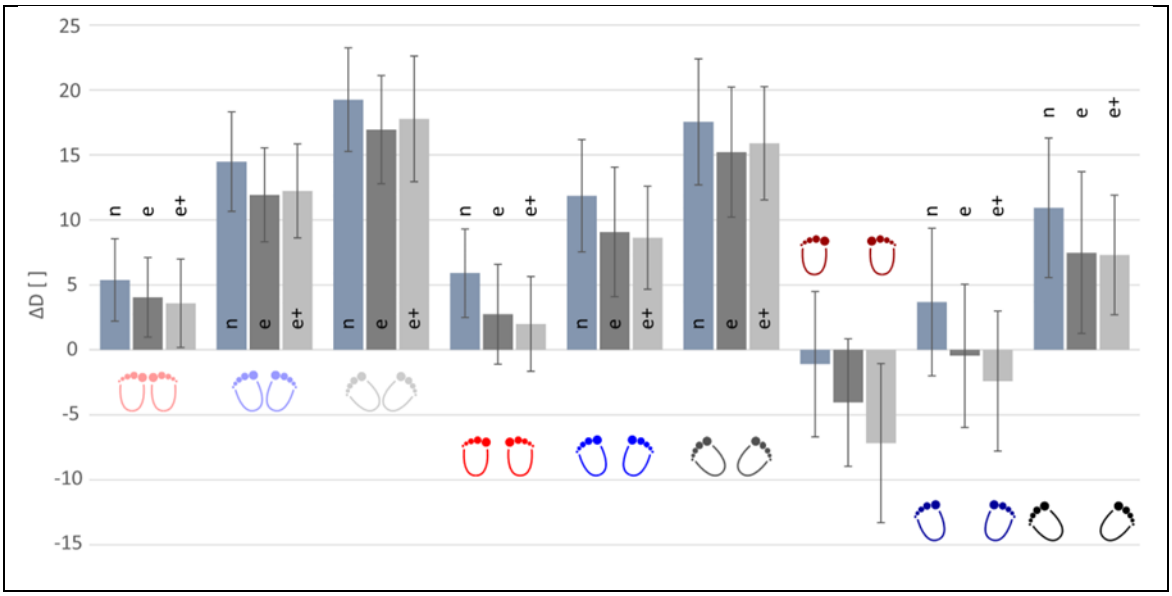

Figure 8. Averaged values including standard deviation ΔD* [% of leg length] displayed for the novice squatter (n), the experienced squatter non-loaded (e) and loaded (e+), for all three stance widths and all three feet placement angles. ΔD* is significantly different between the different stance widths, feet placement angles and between the three groups. While an increasing angle in feet placement angle led to an increasing ΔD*, an increased stance width resulted in a decreased ΔD*. Novice squatters showed a higher ΔD*, while additional weight provoked a smaller ΔD* (Lorenzetti et al. 2018.)

In order to reduce the risk of injury, the position of the knees during squat exercise is generally recommended to remain vertically between the malleoli in the frontal plane, avoiding either medial or lateral knee displacement. Any excessive mediolateral movement of the knee may indicate a functional deficit, such as a reduced ROM of the ankle joint which leads to valgus positions of the knee. However, there are other factors such as femoral and tibial longitudinal rotation and the stance width of the squat. Figure 8, illustrates the results summarised in a series of box plots. The study found that in general, knee varus (negative standard deviation) is much more common that valgus. The greater degree of varus in novice squatters was therefore expected (Lorenzetti et al., 2018.)

3.7 Exercise classification

Back squat exercise involves the movement of several body segments, shank, thigh, sacrum, spine and head. Monitoring the movement of several body segments cannot be achieved with a single sensor in a smart phone or smartwatch, hence the need for several IMMU sensors worn on individual body segments (Shen et al., 2018; Chang et al., 2007; Cheng et al., 2013). Monitoring the quality of squats is particularly challenging, one study implemented a system comprising of several EMG sensors to monitor which muscle sets engaged (Mokaya et al., 2015). An alternative system utilised RFID tags on dumbbells, FEMO platform (Ding et al., 2015). Smartwatches sense wrist orientations and partial torso movements, the MiLift system utilised a single smartwatch with accelerometer and gyroscope sensors to classify several upper body exercises (Shen et al., 2018). The MiLift system employed sensor fusion of accelerometer and gyroscope data to create a gravity sensor. The gravity sensor extracts

the gravity component from the body segment movement acceleration, to create a signal closer to the ground truth signal, resulting in superior device orientation.

Non-automatic workout tracking apps require the user to manually start/stop the tracking of each set of reps and/or workout session. To detect activity transitions and identify the start of exercise and would require a two-stage classifier. First a light-weight low power algorithm to detect high-level changes, such as walking, and weightlifting. The second stage classifier is selected when squats are detected and detailed analysis of squat quality is required. This approach is motivated by previous studies which utilised hierarchical classifiers (Khan et al., 2010; Zhang et al., 2010; Shen et al., 2018; Xu et al., 2011).

Google´s activity recognition client is able to detect still, on foot, walking running, cycling, in vehicle, tilting relative to gravity (Google Developers, 2019). The client conserves power and is periodically awaken, to perform short bursts of sensor data analysis. The android activity client returns a value from 0 to 100 indicating the likelihood that the user is performing a particular activity. The larger the value, the more consistent the data used to perform the classification is with the detected activity. Larger values indicate a greater likely-hood that the detected activity is correct, while a value of <= 50 indicates that there may be another activity that is just as or more likely.

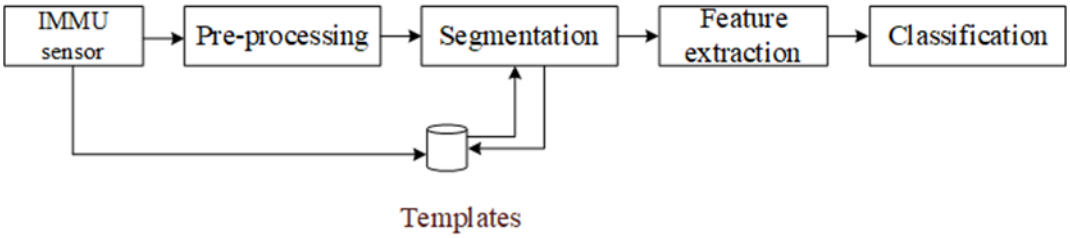

Figure 9. Inertial Measurement Unit based exercise classification system (O'Reilly et al. 2017)

The aim of exercise tracking is to record the number of sets in a workout session. Where each set is a number of repetitions of the exercise. An aim of this study is to record the number of repetitions of back squats in each set. In order to quantify the quality of each back squat repetition, using ideal ROM as a metric, the method would compare the depth of the depth of the back squat in the sagittal plane, by comparing absolute angle positions of the thigh at the start and mid cycle of the back squat. In mobile computing, processor resources are limited by the smartphone processor. Bluetooth Low Energy local wireless connectivity with 2Mbps bandwidth and 5G cloud connectivity with sub one millisecond latency, make cloud-based signal processing, activity classification and machine learning feasible.

4. Methods

4.1 Overview of study design

The study is conducted within a design science research framework, where the artefact under construction is subject to relevance and rigor cycles. The relevance cycle utilises a qualitative methodological framework following the interpretive paradigm. The study ontology being constructivism and the epistemology, interpretive relativism. The interpretive paradigm it is prone to issues due to several principles; the principle of interaction between researcher and subjects, the principle of abstract generalization, and the principle of multiple interpretations (Klein and Myers, 1999). In the relevance phase of the study a system is proposed for the monitoring of patient exercise with wearable sensors. Ideal kinematic data acquired with a commercial motion capture system, is presented to illustrate the capabilities of the proposed system. The interviews are conducted with physiotherapists in two fields of practice, general musculoskeletal and post-operative physiotherapy.

Qualitative research is founded on the principle that data analysis should be conducted simultaneously with data collection (Coffey and Atkinson, 1996). A study with several interviews is able to progressively focus interview questioning and observations, as decisions are made in the testing of emerging conclusions (Maxwell, 2008). The merit of an unstructured interview lies in its conversational nature, which allows the interviewer to be highly responsive to individual differences and situational changes (Patton, 2002). To be responsive and collect the required responses requires the interviewer to have skills in listening and in leading the conversation. Opening the interview with a general question which invites the interviewee to take over and lead the conversation, followed by more probing focused questions which lead the conversation to the desired areas of focus (Zhang and Wildemuth, 2009).

In the rigor phase of the study methods suitable for the construction of a back squat classifier are sought. The main areas of interest being biomechanical analysis of squat exercise, and activity recognition and gait analysis. Squat exercise recognition being expanded to included power lifting squats where Escamilla et al. (2001b) utilised a six stage analysis of squats in power lifting using angular velocity. Other approaches exist for squat analysis, of which the six stage approach best suited the data in this study.

The methods utilised for analysis of kinematic data are taken from biomechanics, including the calculation of the first and second derivatives of absolute angular position. Whereas analysis of the motion of a power lifting bar during squat exercise by Escamilla et al. (2001b) uses angular velocity of the lifting bar, this study applies angular velocity of the sacrum, thigh and shank to the exercise classifier. The second derivative being utilised with Fourier transform reveal squat time period, a value used to segment data in the process of identifying the start of the back squat cycle. A single-case mechanism experiment in validation research is a test where a stimuli is applied to a validation model and the response is explained by mechanisms internal to the model (Wieringa, 2014). In this study, back squat kinematic data from a novice athlete is

processed by the OoS, a classifier and appraiser method, the resulting appraisal of which is achieved by several processes within the appraiser method.

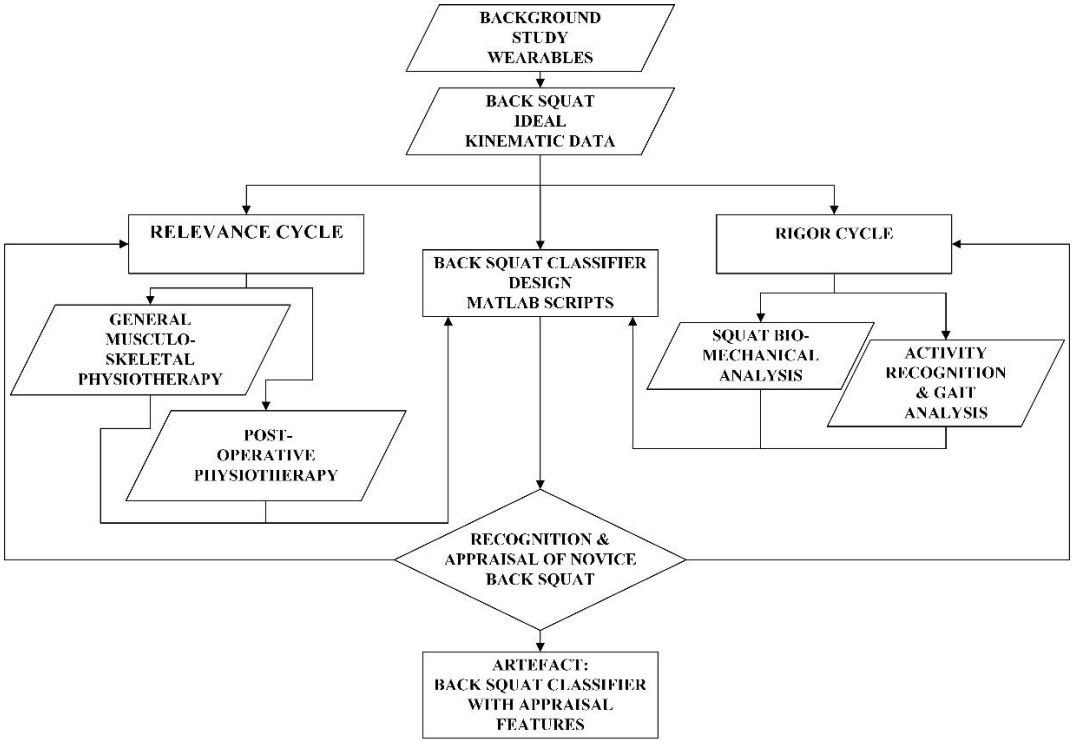

Figure 10. Research design flowchart

4.2 Relevance cycle

In the relevance phase of this study, interviews are conducted with physiotherapists to gain their opinions on the suitability of wearables systems to appraise patient exercise. This stage performs two functions, giving evaluation concerning the system design, and also assessing the problem relevance. The relevance cycle examines the characteristics of people, their roles and how they interact with information systems. The option of taking notes, as opposed to voice recorder is always offered to interviewees and their choice respected. An unstructured interview is chosen as the method for this phase of the study because it allows for the most flexibility, which is beneficial to maintaining a warm rapport with the physiotherapist.

The presentation is given as a means to explaining the relevant technologies on which the proposed system would be designed, including a live demonstration of a Texas Instruments SensorTag wireless Bluetooth Low Energy (BLE) IMMU sensor with graphical app display of real-time motion data. The presentation ends with plots of IMMU data captured during squats exercise with, non-wireless sensors. The plots of knee angle against angular velocity give a visual representation of how an exercise activity recognition algorithm would recognise and appraise patient performance during squats exercise.

Table 2. Questions answered through discussion

#	**Question**
1	Is mobile technology an obstacle for patients?
2	Is ideal range of motion (ROM) a useful metric?
3	Should the physiotherapist set the ideal ROM?
4	Real-time back squat ROM feedback useful?
5	Is a histogram of ROM range per set of back squats useful?
6	Is there benefit in a wearable motion capture App to aid learning squats?
7	Other feedback?

Immediately following the presentation, the interview is opened by asking a very general question, if smartphones were used by most patients? Once the interviewee has gained confidence by discussing smartphone use, the conversation moves to the idea of the app using ideal ROM as a metric. The discussion is unscripted, with the aim of answering areas of interest at the pace of the interviewee and generating as much discussion as possible, the aim to gain detailed answers to the seven questions in Table 2.

The test presentation followed by a group interview, is used as a pilot study conducted with a class of twenty-six students of physiotherapy. The pilot study is a useful test before applying the method to practising professional physiotherapists. The pilot presentation answers any concerns with the technical level of the presentation, and which areas of the presentation generated the most interest. Immediately following the presentation, the unstructured group interview with the students commences. First, asking general questions before leading the conversation towards the idea of using ideal ROM as a metric for the app. After the group interview, the students give anonymous feedback via a virtual Padlet wall, (Appendix A). This serves as a simple control against the issue of interaction with the researcher.

The first physiotherapist's presentation and interview is conducted with a senior lecturer of physiotherapy at a Finnish University of Applied Sciences. The lecturer has sixteen years of experience in the practice of musculoskeletal physiotherapy before a career as a senior lecturer. The second presentation is conducted with a physiotherapist qualified to the level of Orthopaedic Manual Therapist (OMT). The practice is situated in a sport centre, giving extensive experience of sports injuries, therapeutic exercise and musculoskeletal physiotherapy. The third presentation is conducted with a physiotherapist qualified to the level of Orthopaedic Manual Therapist (OMT). The practice provides physiotherapy services to the city soccer team, with extensive experience of sports injuries, sports physiotherapy, sports coaching and musculoskeletal physiotherapy.

The fourth presentation is conducted with a team of five physiotherapists qualified to master's degree level in rehabilitation at a central city hospital in Finland. All members

of physiotherapy department are experienced in the long-term rehabilitation of patients following hip and knee total endoprosthesis (TEP). Their interview is conducted purely from the perspective of the long-term rehabilitation of hip and knee TEP patients.

4.3 System description and techniques presentation

The system design utilises IMMU wireless technology in addition to human motion capture and recognition techniques. The study presented the proposed system in the form of a live presentation to describe how the IMMU technology captures human movement through MEMS accelerometers and gyroscopes. Gyroscopic drift errors caused by precession are corrected with accelerometer data, the combination of both sensors in one wearable sensor increases data accuracy. Precession is caused by body segment rotation, the end of the gyroscope furthest along the body segment experiences more centripetal force, accounting for a net force on one end of the gyroscope, the cause of gyroscopic precession. Algorithms including a Kalman filter in the Xsens MTx software compensate for gyro drift with accelerometer data, to give a more accurate value for absolute angle (Zhang and Reindl 2011; Wang, et al. 2011).

Wearable human motion capture systems are explained, and their use illustrated in motion capture data for back squats exercise with time sequenced photographs, and IMMU data from the sacrum, thigh and shank in the sagittal plane. Motion data from only the sagittal plane is selected partly on the basis of a back squat knee alignment study by Lorenzetti et al. (2018) which proved a greater amount of mediolateral movement occurred with less experienced cohorts. With knee movement in the frontal plane being minimal with good exercise technique, the sagittal plane became the main focus with a range of attitude for the thigh and sacrum of over fifty degrees. From literature, Sato & Heise (2012) back squat exercise is characterised as a sagittal plane movement as the lower extremity joints are the primary sources of movement.

No attempt is made in this study to calculate knee varus or valgus. Measurements of changes in absolute angle in the transverse and frontal planes by the IMMU worn on the outer thigh were found to be inaccurate. Throughout one back squat cycle, the thigh transverse plane angle varied by twenty-five degrees, and in the frontal plane by twenty-two degrees. Values in both planes did not corelate to observations made of knee movement. Absolute angle measures of thigh movement in traverse and frontal plane were considered unreliable. The reason for such exaggerated values is considered to be due two possible sources of error. Firstly, the elastic strap which held the IMMU in place, may have required readjustment, since errors were on occasion noticed in the sagittal plane. Secondly, muscle bulge. From literature, Kato et al., (2015) utilising tactile sensors measured muscle bulge movement, derived from muscle contraction. Li et al. (2013) utilised ultrasonic measurements of changes in the cross-sectional plane of the quadriceps muscles. Scheepers et al., (1997) anatomy-based computer modelling, where deformation of muscles due to contraction are represented by changes in ellipsoidal profile. From these studies it could be inferred that the muscles of the outer thigh bulge on contraction, creating a greater curvature to the surface beneath the IMMU sensor. Since the IMMU case dimensions are fifty-three millimetres by thirty-eight millimetres, small relative to the dimensions of the thigh, changes in quadriceps muscle bulge could create significant changes in sensor heading in the traverse and frontal planes.

The system proposal consists of three IMMU sensors used on the shank and thigh, with the third IMMU on the sacrum. The sacrum sensor gives the absolute attitude position of the sacrum, which also indicates pelvic tilt. From literature, Myer et al. (2014), the squat requires sufficient spinal mobility to assume and maintain a slight lordotic posture of the lumbar region. Failure to assume the correct spinal posture may tend to exert excessive pressure to the lower back, especially if the head is tilted forwards as well. The posture of the thoracic spine is described as slightly extended and held rigid. From literature of human anatomy, Kahle et al. (1986), the neutral position of the spine is described with two posteriorly convex curvatures, kyphoses in the sacral and thoracic regions. Without a fourth sensor to describe attitude of the thoracic spine with which to compare with the sacral region, posture of the spine is considered outside of the scope of this study.

The IMMUs one hundred samples per second data is captured using quaternion orientation output, which is converted by the MTx application to Euler angles before being saved in space delimited format text files. The Euler angles produced are the cumulative summation of changes in angular orientation measured by the IMMU gyros at each sample, captured at a sampling rate of 100 Hertz. The kinematic data is processed manually to select one ideal back squat from a series performed by a subject with good technique.

The motion capture data in the sagittal plane, from the three body segments are written to three separate space delimited files. The three files are manually imported in to three spread-sheets for editing. After import into the spread-sheet, extra columns of data are calculated for the angular velocity and angular acceleration using the first central difference method (FCDM). After editing, only the data for the second squat, the deepest squat with good technique remains from the original sequence of six. The edited spreadsheets are then exported to space delimited text files named 2nd squat for sacrum, thigh and shank. The three files, in space delimited form are now suitable to allow import, and plotting of kinematic data against time by Matlab (version R2019a, The MathWorks Inc., Natick, MA, USA).

The Matlab script to plot the kinematic data for relative change of angle for body segments sacrum, thigh and shank (Figure 13) is listed below in Figure 11.

```
SH=dlmread('MT_00130431_011-000_2ndsquat_SH.txt');
TH=dlmread('MT_00130431_011-001_2ndsquat_TH.txt');
SA=dlmread('MT_00130431_011-002_2ndSquat_SA.txt');
%calculate starting point of 2nd squat
% SHank, THigh and SAcrum start at sample 19264,
x=SH(:,1);
x=(x-19264); % 011-000.txt sample counter starts at 19264
y=SH(:,3);  % SHank X axis
y=(y-82.87); % subtract SHank start/rest angle 82.87°
y2=TH(:,3); % THigh X axis
y2=y2-65.01; %subtract THigh start angle 65.01°
y3=SA(:,3); % SAcrum X axis
y3=y3-76.63; %subtract SAcrum start angle 76.63°
plot(x,y,'g', x,y2,'r', x,y3,'b' );
xlabel('time increments 1/100 second');
ylabel('2nd Squat SHANK Green, THIGH Red, SACRUM Blue Gyro Pitch,
Deg');
print ('Gyro X', '-dtiff', '-r600')
```

Figure 11. Matlab script – plot change in absolute attitude sacrum, thigh, and shank

Data from the three body segments contained in three space delimited text files, are assigned the labels “SH” for shank, “TH” for thigh, and “SA” for sacrum. The percentage character at the start of a line indicates a comment line which is not executed by Matlab. The percentage character is also used for comments after a line of code. Comments aid human comprehension of the code. The sample number and therefore the time progression, in the first column of the delimited text file, is assigned to the x axis by line 6 of the script. Matlab reads the delimited file like an array and the colon denotes select all rows, followed by a comma, then the first column is selected by the integer value one. The value of x is subtracted by 19264, since this is the number of samples taken before the selected squat, the second squat of the sequence from the original capture file. The percentage character indicates the start of comments, which are not interpreted by Matlab.

The shank absolute angle in the sagittal plane is recorded in column three of the delimited text file 'MT_00130431_011-000_2ndsquat_SH.txt' which is assigned label SH. This value is the y value of the plot. The y value is read by line eight of the script, where y equals the values in column three of the array, all the rows of column three, denoted by the colon. The absolute value for the angle in the sagittal plane at sample 19265 is 82.87 degrees, is at the start of the back squat exercise. This absolute angle is subtracted from y, so that the plot commences from zero. The reasoning, to aid visualisation by human eyes of the relative segment motions, commencing all three segments from the same reference of zero degrees.

The script continues with the thigh segment which is plotted as value y2. The thigh data is contained in the delimited text file assigned label TH, where the absolute angle in the sagittal plane is contained in column three. The code to read the sagittal thigh angle is in line ten. All row values of the array are read due to the colon wildcard, and the column is selected by the integer three. The sagittal absolute angle at sample 19265 is 65.01 degrees, measured to the horizon, which in line eleven is subtracted so that the thigh plot also starts at zero degrees. The same method is then repeated for the sacrum which takes variable y3. Line fourteen executes the plot command. The plot command options syntax are within parentheses, where the variable y for the shank is plot in green. The variable y2 for thigh, is plot in red, and the variable y3 the sacrum is plot in blue. The label for the x and y axis’ are defined in lines fifteen and sixteen. Line seventeen defines the print options, file name ‘Gyro X’, the type of plot being TIFF, and the resolution of six hundred dots per inch. The plots are drawn in Figure 13, above which Figure 12, displays a time sequence set of 5 images illustrating a back squat exercise repetition.

The IMMU data from the Xsens MTx application for one squat repetition in the sagittal plane is imported in to Matlab to create the plot of relative change in body segment angle against time shown in Figure 13. All three body segments, sacrum in blue, thigh in red and shank in green are displayed in the same axis to illustrate the unique plot or ‘signature’ created by each body segment during the back squat exercise.

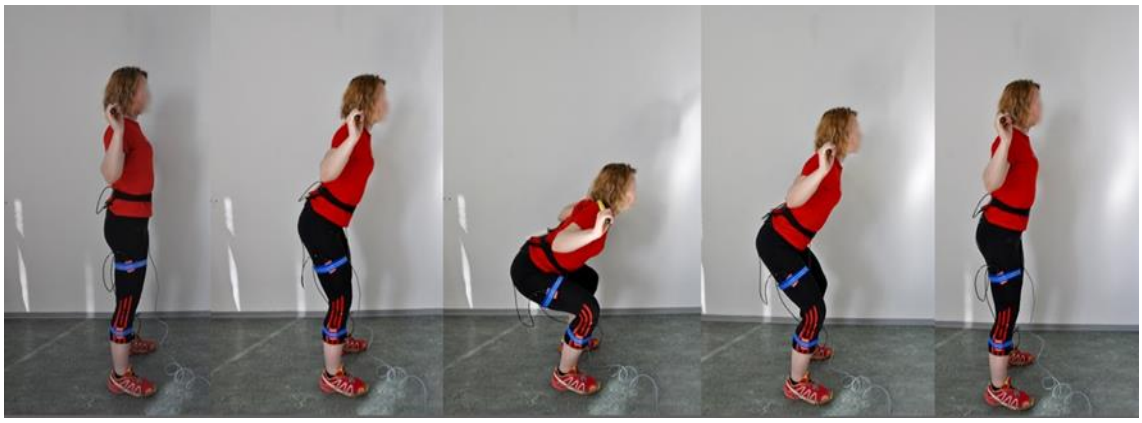

Figure 12. Back squat exercise with wearable sensors time sequence.

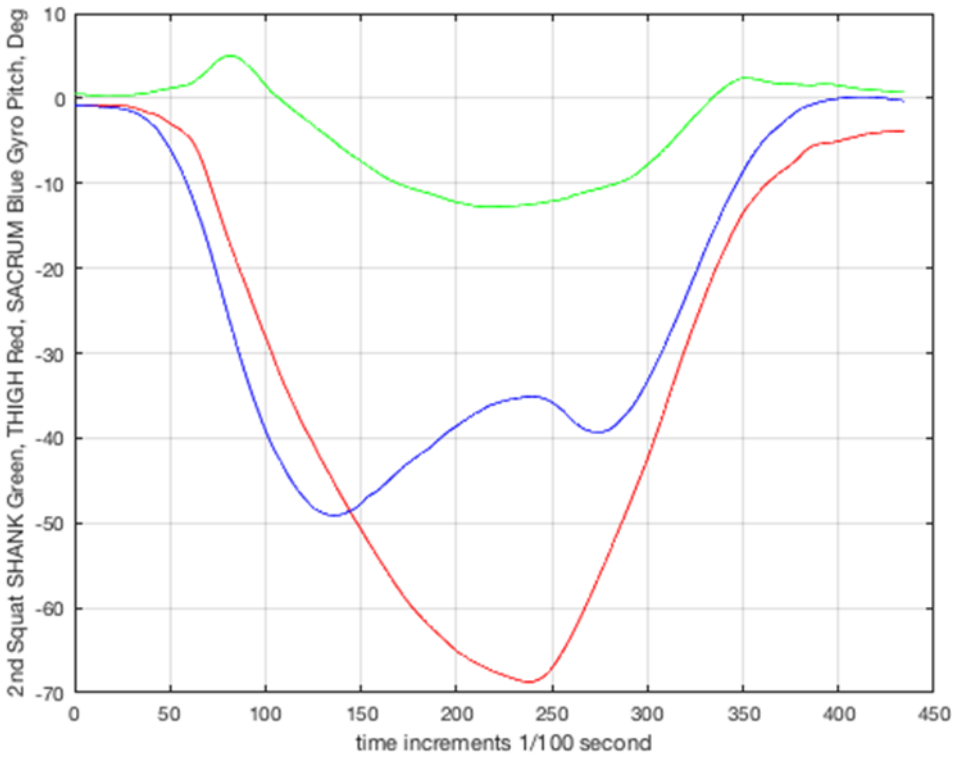

Figure 13. Sagittal plane back squat exercise IMMU motion capture, relative change in absolute angle (degrees) of body segments against time in 1/100 second samples. Sacrum blue, thigh red, shank green.

The segment plot of relative change of absolute angle (Figure 13) could be utilised by a decision tree algorithm, however, the number of gradient changes is less than in the plot of angular velocity (Figure 14). When the IMMU data is further processed to create angular velocity of body segments, the number of gradients and gradient direction (sign +/-) changes increases. With the thigh segment there are two distinct gradients in the negative cycle and two gradients in the positive cycle. The gradient in the thigh descent cycle changes direction from negative to positive, and in the ascend cycle the gradient changes from positive to negative

The change in gradient direction, negative to positive, and positive to negative at distinct stages of the back squat exercise give the thigh angular velocity data a strong "signature". Changes in the gradients of angular velocity correspond to key "stages" of segment kinematics throughout the back squat cycle. Gradients of angular velocity could be analysed by a decision tree algorithm to recognise the kinematic data as back squat exercise and to use slope gradient and duration to qualify the back squat range of motion.

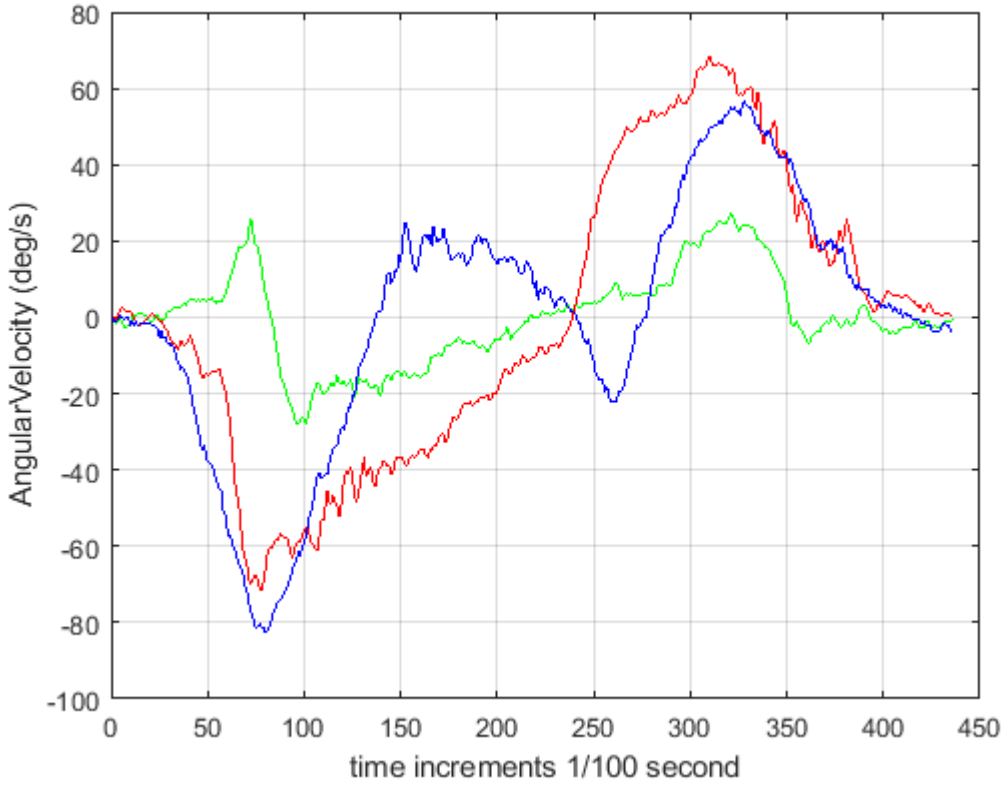

Figure 14. Sagittal plane back squat exercise IMMU motion capture, angular velocity (deg/s) of body segments against time. Sacrum blue, thigh red, shank green.

Angular velocity slope gradient and duration reduces the burden of the motion capture system to maintain the accuracy of absolute angle within the earth frame orientation. If the IMMU is not accurately aligned with the thigh, then there will be an error in the absolute angle of the body segment. This is not critical since even while moving out of alignment, the IMMU captures the changes in angular velocity from which angular

velocity is derived. Thus, by time duration, the angle through which the thigh traversed can be calculated.

The Matlab angular velocity script below plots the new data from calculations performed on absolute angle when the IMMU kinematic data is imported into spreadsheets. The resulting space delimited text files have additional columns that contain angular velocity and angular acceleration of the body segments. Angular velocity is calculated by finding the difference between two samples and dividing by the time period between the two samples, using the first central difference method.

The Matlab script to plot the kinematic data for angular velocity from sacrum, thigh and shank (Figure 14) is listed below in Figure 15.

```
clear all;
close all;
clc
SH=dlmread('MT_00130431_011-000_2ndsquat_SH_CDM.txt');
TH=dlmread('MT_00130431_011-001_2ndsquat_TH_CDM.txt');
SA=dlmread('MT_00130431_011-002_2ndSquat_SA_CDM.txt')
% SHank, THigh and SAcrum start at sample 19264
x=SH(:,1);  % sample #,dlm file column 1
x=(x-19263); % 011-000.txt sample counter starts at 19264, sample #1
y=SH(:,7);  % SHank sagittal plane angular velocity
y2=TH(:,7); % THigh sagittal plane angular velocity
y3=SA(:,5); % SAcrum sagittal plane angular velocity
plot(x,y,'g', x,y2,'r', x,y3,'b' );
xlabel('time increments 1/100 second');
ylabel('2nd Squat SHANK Green, THIGH Red, SACRUM Blue
AngularVelocity, Deg/s');
print ('Gyro X', '-dtiff', '-r600')
```

Figure 15. Matlab script – Plot sagittal plane angular velocity sacrum, thigh, and shank, in degrees per second

The absolute angle of a body segment, theta (θ), is calculated for successive positions in time as angular displacement (Δθ).

$$\Delta\theta = \theta_{final} - \theta_{initial} \qquad (8)$$

Angular velocity is the first derivative of angular displacement. Representing the gradient of the tangent to the plot of angular displacement, gives the instantaneous value for angular velocity. Characterised by the Greek letter omega (ω), angular velocity is a vector quantity that describes the rate of change of angular position with respect to time.

$$\omega = Change\ of\ angular\ position\ /Change\ in\ time$$

$$\omega = \theta_{final} - \theta_{initial}/time_{final} - time_{initial} \qquad (9)$$

The method to calculate angular velocity applied to data obtained over a time series of samples of a kinematic analysis is the first central difference method (FCDM). The method calculates the angular velocity at the same instant as the angular position. Described in equation (10) where the angle θ_i is the initial angle at t_i the initial time (Hamill and Knutsen 2006.)

$$\omega = \theta_{i+1} - \theta_{i-1}/t_{i+1} - t_{i-1} \qquad (10)$$

Angular acceleration is the second derivative of angular displacement. Representing the gradient of the tangent to the plot of angular velocity, gives the instantaneous value for angular acceleration. Characterised by the Greek letter alpha (α), angular acceleration is a vector quantity that describes the change of angular velocity with respect to time.

$$Angular\ acceleration = Change\ in\ angular\ velocity / Change\ in\ time$$

$$\alpha = \omega_{final} - \omega_{initial} / time_{final} - time_{initial} \quad (11)$$

$$\alpha = \Delta\omega / \Delta t \quad (12)$$

In kinematic analysis the usual method of calculating angular acceleration is again the central difference method as described in equation (13). For ease of understanding, biomechanists generally present their results in degrees per second squared (deg/s^2), but the most appropriate unit for angular acceleration is radians per second squared (rad/s^2) (Hamill and Knutsen 2006.)

$$\alpha_i = \omega_{i+1} - \omega_{i-1} / t_{i+1} - t_{i-1} \quad (13)$$

Processing of the motion capture data produces a plot of knee angular velocity against knee angle, plot with a black line (Figures 16 & 17). Knee angle in the sagittal plane is measured between posterior thigh and shank segments. This measurement is of interest to physiotherapists as ROM of the knee gives a good indication of knee health and the knee joint, which has a high injury potential. According to Hamill and Knutsen (2006), the knee joint is a frequently injured area, depending on the sport, accounting for 25% to 70% of reported injuries. In males aged 20 to 29 years, most knee injuries were associated with soccer and skiing.

At the start of the back squat, knee angle is around 150 degrees since both the shank and thigh are near vertical. At the lowest point of the back squat at the end of the descent phase, the knee angle is smallest, around sixty-five degrees. The descent plot of knee angle against angular velocity (Figure 16) is read from right to left because at time zero, knee angle on the x axis is at its maximum. The ascent plot (Figure 17) is read from left to right, since the ascent phase of the back squat starts with knee angle at its minimum value.

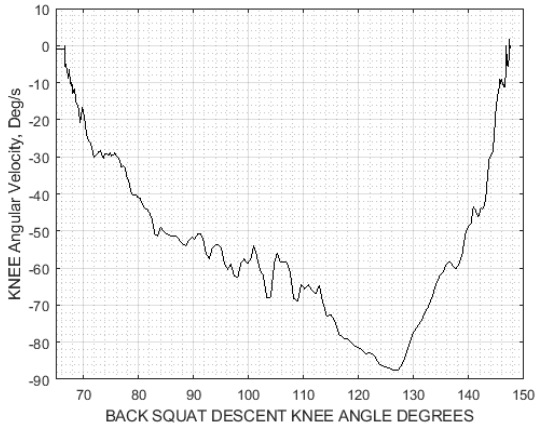

Figure 16. Back squat descent knee angular velocity (deg/s) against knee angle in degrees

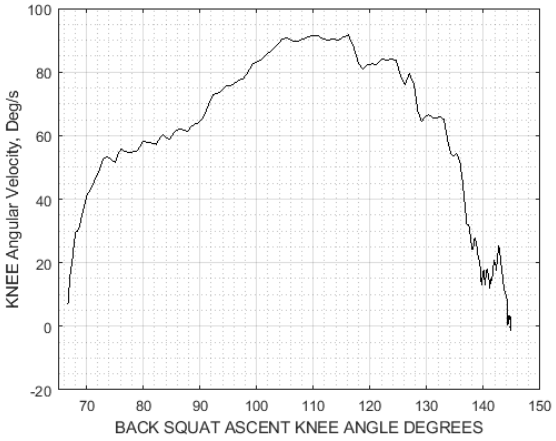

Figure 17. Back squat ascent knee angular velocity (deg/s) against knee angle in degrees

The proposed apparatus for monitoring back squats consists of three wireless Bluetooth Low Energy (BLE) IMMU sensors, one worn on a belt over the sacrum and a second IMMU worn on an elastic strap on the outer thigh and a third worn on the outer shank. During the presentation a wireless wearable IMMU is demonstrated, a Texas Instruments CC2650STK (Figure 18) weighing 62grams, transmitting 9 degrees of freedom motion data, accelerometer, gyroscope, magnetometer all in three dimensions via Bluetooth Low Energy to an Android App in real time.

Figure 18. Texas Instruments CC2650 Sensortag (Texas Instruments, 2015)

The graphical display of acceleration, and rotation in three axis' proved the IMMU data could be processed by a smartphone. However, it is a simple BLE IMMU demonstration app, with no specific application to human activity recognition, and a sample rate of only ten Hertz.

Wearable sensors are by no means perfect and some of the practical issues that need to be resolved before a fully functional system could be deployed were high-lighted. Human motion capture in the gym is a challenge with distortion of the geomagnetic field due to the large quantity of iron barbells and steel exercise machines. In the process of creating the motion capture traces for the presentation, equipment in the gym close to the shank MTx sensor distorted magnetometer readings in the frontal plane, such that rotational reading spun through 180°between two samples, then reverted back to the correct heading in the following sample. By exercising more than three meters away from large training machines, the problem is resolved. There are issues with ergonomics, where the IMMU sensor on the outer thigh slips in vertical alignment throughout the set of squats, rotating over 30° from vertical, (Figure 19). The rotation of

the wearable sensor causing the start angle of each repetition to gradually decrease from 85° to 55° from horizontal.

Figure 19. Ergonomic issue securing IMMU to outer thigh

Re-securing the elastic strap, temporarily resolves the issue. Figure 19 is used in the presentation to good effect as the audience of physiotherapists appear to have ideas regarding the best strapping system to use when securing a sensor to the outer thigh. This is one area of the presentation that appears to raise interest with physiotherapists. Studies into the effect and compensation of soft tissue artefact (STA) on markers for human movement analysis with stereo photogrammetry, concluded that STA is the most significant source of errors, and suggested research into structural models that would allow calibrated compensation (Leardini et al., 2005).

The use of a double knitted wearable goniometer utilising IMMUs and knitted piezo resistive fabrics (KPF), to measure knee angle is the subject of a study by Tognetti et al., (2015) (Figure 20). Sensors are fused through a Kalman-filter based algorithm which achieved errors of less than two degrees.

Figure 20. Prototype double layer knitted knee joint wearable goniometer (Tognetti et al., 2015)

Without a working app to demonstrate to the audience, several screen icons give an impression of how the app may give visual feedback based on ideal ROM. The app icons in Figure 21, attempt to give visual measures on squat depth and posture. The

audiences appear to have no problems interpreting their meaning, which suggests the features of the system functionality to be developed are relevant.

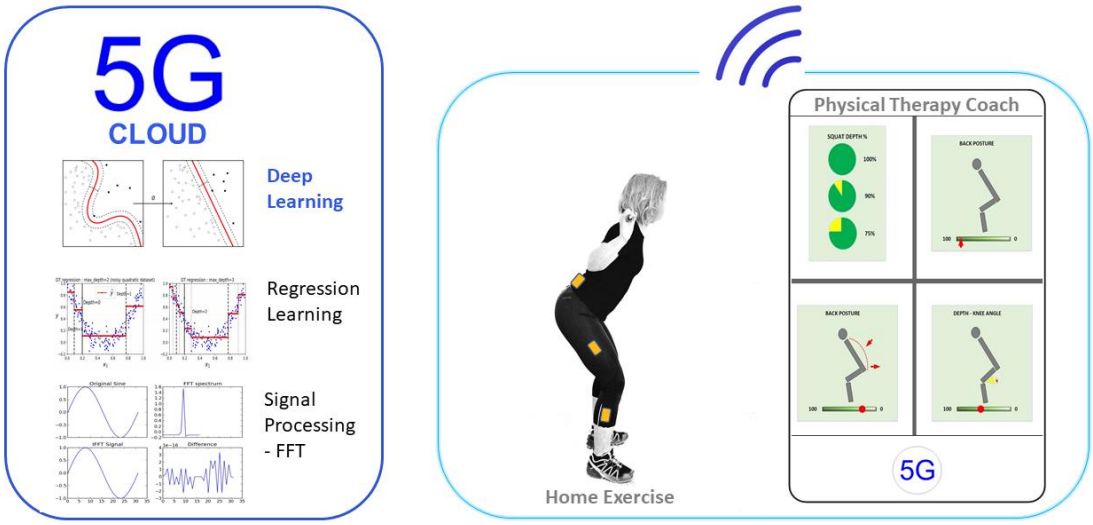

Figure 21. App icons for ROM and posture with 5G cloud service

The app icons indicate how it acts as a tool to make learning good back squat technique easier by performing real-time measurements that form the basis of technique appraisal. The presentation then dovetails into an interview with the physiotherapist to gain opinions on the perceived suitability of the system. The discussion covered the seven key questions concerning the system design, as described in Table 2. The summary of questions answered on the suitability of inertial wearable sensors for exercise appraisal are shown in Table 3.

Table 3. Summary of system suitability in physiotherapy

Question	**Physio Students**	**Physio1**	**Physio2**	**Physio3**	**Post-op Physios**
Is mobile technology an obstacle for patients?	NO	NO	NO	NO	YES
Is ideal range of motion (ROM) a useful metric?	YES	YES	YES	YES	NO
Should the physiotherapist set the ideal ROM?	YES	YES	YES	YES	NO
Is real-time back squat ROM feedback useful?	YES	YES	YES	YES	NO
Is a histogram of ROM range per set of back squats useful?	YES	YES	YES	YES	NO
Would a wearable motion App aid learning squats?	YES	YES	YES	YES	NO
Other feedback given?	YES	YES	YES	YES	YES

From the summary of system suitability, it is not received well by post-operative physiotherapists because ROM is not considered in patient recovery. The primary concern being maximum load bearing weight that the leg is able to support, which is assessed by the surgeon. However, general musculoskeletal physiotherapists considered the system useful for patients learning good back squat technique, and in the early detected of recovery issues.

4.4 Initial kinematic data analysis

Following the interviews with practicing physiotherapists, analysis of back squat kinematic data is conducted to develop methods of measuring the characteristic attributes. From the set of six back squats, the kinematic data is analyzed to reveal variations in motion between individual repetitions.

Table 4. Back squat times

Back squat rep. #	Thigh descent time (s)	Normalized thigh descent time	Thigh ascent time (s)	Normalized thigh ascent time	Thigh descent + ascent time (s)
1	2.64	1	1.98	0.53	4.62
2	2.38	0.5	1.97	0.52	4.35
3	2.46	0.65	1.80	0.19	4.26
4	2.22	0.19	2.22	1	4.42
5	2.12	0	2.21	0.98	4.37
6	2.37	0.48	1.70	0	4.07

Table 5. Back squat descent angles

Back squat rep. #	Thigh start angle (deg. to horizontal)	Thigh lowest angle (deg. to horizontal)	Thigh descent angle range (deg.)	Thigh normalized descent angle range (0 to 1)
1	66.262	-0.597	66.859	0.925
2	64.099	-3.711	67.810	1
3	61.157	-0.601	61.758	0.525
4	60.571	1.950	58.621	0.279
5	59.380	2.287	57.093	0.159
6	61.421	6.355	55.066	0

Table 6. Back squat ascent angles

Back squat rep. #	Thigh ascent start angle (deg. to horizontal)	Thigh ascent highest angle (deg. to horizontal)	Thigh ascent angle range (deg.)	Thigh normalized ascent angle range (0 to 1)
1	-0.597	64.115	65.309	1
2	-3.711	61.159	64.870	0.947
3	-0.601	60.571	61.172	0.507
4	1.950	59.756	57.806	0.106
5	2.287	61.421	59.134	0.204

6	6.355	63.272	56.917	0

Tables 4, 5 & 6 illustrate that angle range and time duration for back squat ascent and descent is not equal and are unique for each back squat. Although repetition number 2 has the deepest angle traversed on descent, on ascent the angle traversed is less than in the first repetition. To aid visualization of the uniqueness of each squat in a set of six reps, box plots show the median and up and lower quartile range. To create box plots of the thigh descent and ascent angle range traversed, a Matlab script is written. The Matlab script below (Figure 22) creates a boxplot for back squats ascent and descent phase, the angle traversed by the thigh.

```
% data from sequence of 6 squats
% THdes_grange - Thigh descent angle traversed in degrees
THdesc_degrange = [66.859 67.81 61.758 58.621 57.093 55.066];
%THasc_degrange - Thigh ascent angle traversed in degrees
THasc_degrange = [65.309 64.870 61.172 57.806 59.134 56.917];
boxplot ([THdesc_degrange(:), THasc_degrange(:)])% Boxplot the data
% from all columns of array THdesc_degrange
% and THasc_degrange
ylim([54, 70]) % plot y-axis from 54 to 70 deg
ylabel('Thigh angle of traversal - degrees');
set (gca, 'XTicklabel', {'Thigh descent', 'Thigh ascent'})
% label both boxplots on x-axis
```

Figure 22. Matlab script - boxplots for six back squats thigh angle traversed – descent compared to ascent

In the Matlab script above (Figure 22) the angles traversed by the thigh are listed in two arrays, THdesc_degrange, and THasc_degrange. In line nine, the boxplot function reads the colon in parenthesis after each array name which indicates that all columns of the array are to be used as input into the boxplot function. Square parenthesis inside round parenthesis indicate that both boxplots are plot “shoulder to shoulder” in the same figure. The output from this Matlab boxplot script is found in Figure 23.

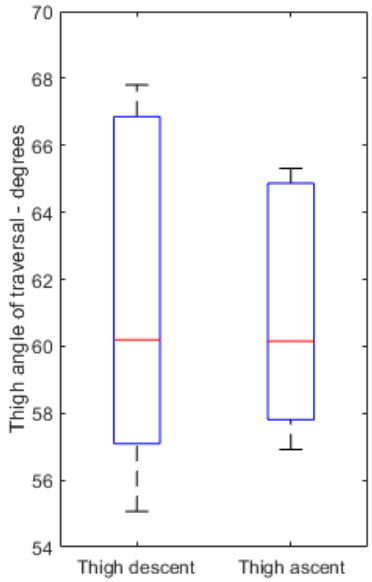

Figure 23. Boxplot six back squats thigh descent and ascent angle (deg).

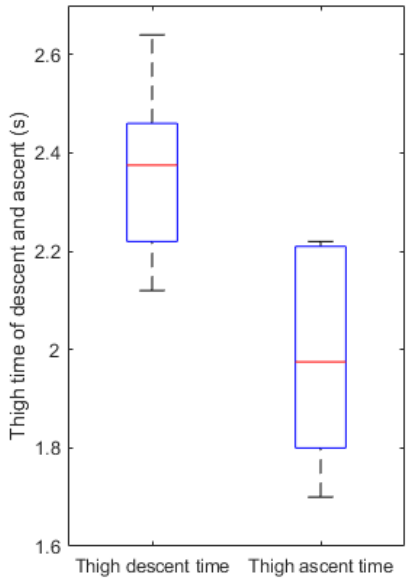

Figure 24. Boxplot six back squats thigh descent and ascent time (s).

The two box plots in Figures 23 and 24 use data from tables 4,5 and 6, which show that angle range traversed by each squat is not identical, in both the descent and ascent phase. In some reps the thigh does not return to as high an angle as the initial starting position. The descent and ascent phases are neither equal, nor invariant. The mean time for descent is longer than the mean time for ascent. This may be due to the technique or fatigue in the person exercising, but also it could be due to movement of the IMMU sensor on the thigh, which is secured only with an elastic strap. The set of six reps has a fairly even rhythm (Table 4), with the time difference between shortest at 4.07 seconds

and longest at 4.62 seconds being only 0.55 of a second. The two boxplots in Figure 24 illustrate that the time for the descent and ascent motions of the thigh are not always equal. To create a successful exercise classifier for back squats, the detection algorithm must be able to allow for these differences in angles and times of the descent and ascent stages.

4.5 Rigor cycle

Rigor cycles in DSR examine data analysis techniques, methods, constructs and frameworks that exist in the knowledge base. The purpose is to use what is already available in the knowledgebase to good effect in constructing a new artefact. To classify back squats from IMMU data requires identification of the start of the exercise cycle. This is something of a challenge since the time period of each back squat exercise is unique. Other exercise classifiers used to recognise human gait such as walking use a combination of accelerometer data and gyroscope data. When the heel first makes contact on the ground, there is a large spike in negative acceleration, which is the signature event in the algorithm to identify the start of the step (Zebin, 2018). Event detection in back squat kinematic data does not have a heel strike event, since the athlete does not perform ambulation. This study utilises gyroscope data alone for exercise recognition. The patterns of changes in direction and gradient of angular position, velocity, and acceleration are the data by which the classifier must operate.

Once the start and end of the back squat is found in the data segment, only then is kinematic analysis of the exercise repetition possible. Typically activity classifiers utilise a method of data segmentation and a sliding window technique to search for the start of an activity O'Reilly et al. (2017). From literature (Alexander and Jayes, 1980), analysed human gait data generated from a floor composed of force plates. The force plates gave acceleration of the subject against time. The changes in acceleration once applied to a Fourier transform, reveals accelerations in the frequency domain, which match individual components of gait.

This study calculates angular acceleration from the thigh using the first central difference method (FCDM) of angular velocity. Then, analysis with Fast Fourier Transform (FFT) converts changes in amplitude in the time domain to changes in amplitude in the frequency domain. The peaks in the frequency domain indicate the presence of cyclic motion. An appropriate window function is selected with the FFT transform to aid frequency resolution, and give a more accurate value of the back squat cycle. The figure below illustrates the flow of gyroscope data within the back squat classifier algorithm.

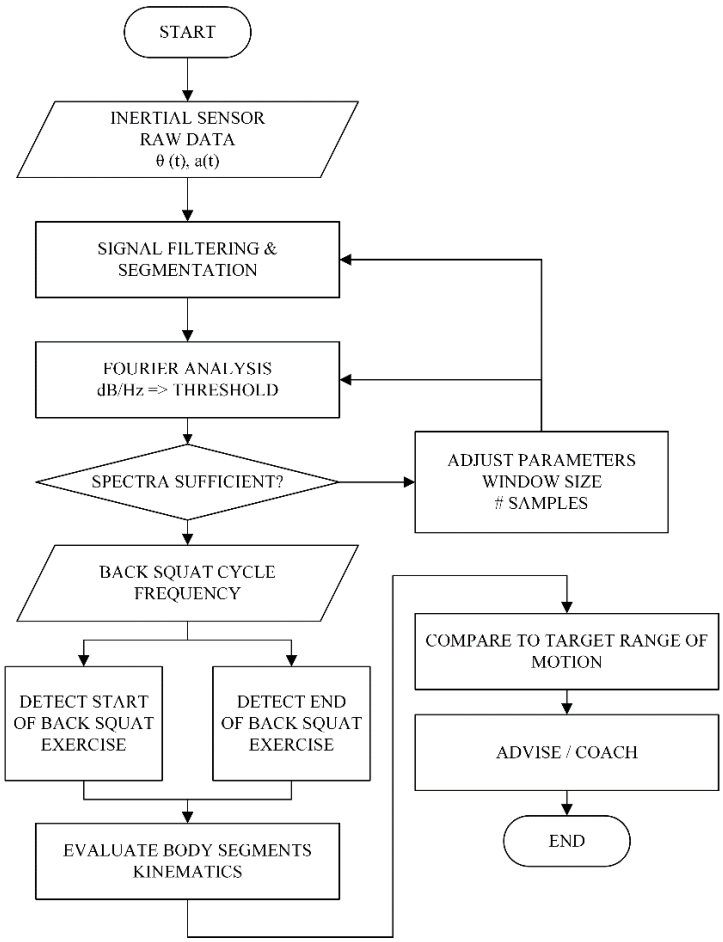

Figure 25. Inertial data signal processing workflow

4.6 Classifier construct

From the plot of angular velocity against time of sacrum, thigh and shank (Figure 26), it is evident that the gradients of the plots are steeper than with absolute angle against time, and for the thigh, there are twice as many gradient directions; two in the decent cycle where the thigh moves downwards with negative angular velocity and two in the ascent cycle where the thigh moves upwards with positive angular velocity. In angular velocity, sign indicates direction, positive for up and negative for down. Positive angular velocity, the portion of the plot above the x-axis, indicates that the thigh is moving upwards. Negative angular velocity, the portion of the plot below the x-axis indicates that the thigh is moving downwards.

The change in the gradient sign of angular velocity indicates if the body segment is accelerating or decelerating. The value of the gradient of angular velocity indicates the degree of angular acceleration. From the changes in gradient sign of angular velocity, (negative to positive or vice versa), six distinct stages of the back squat exercise are clearly visible.

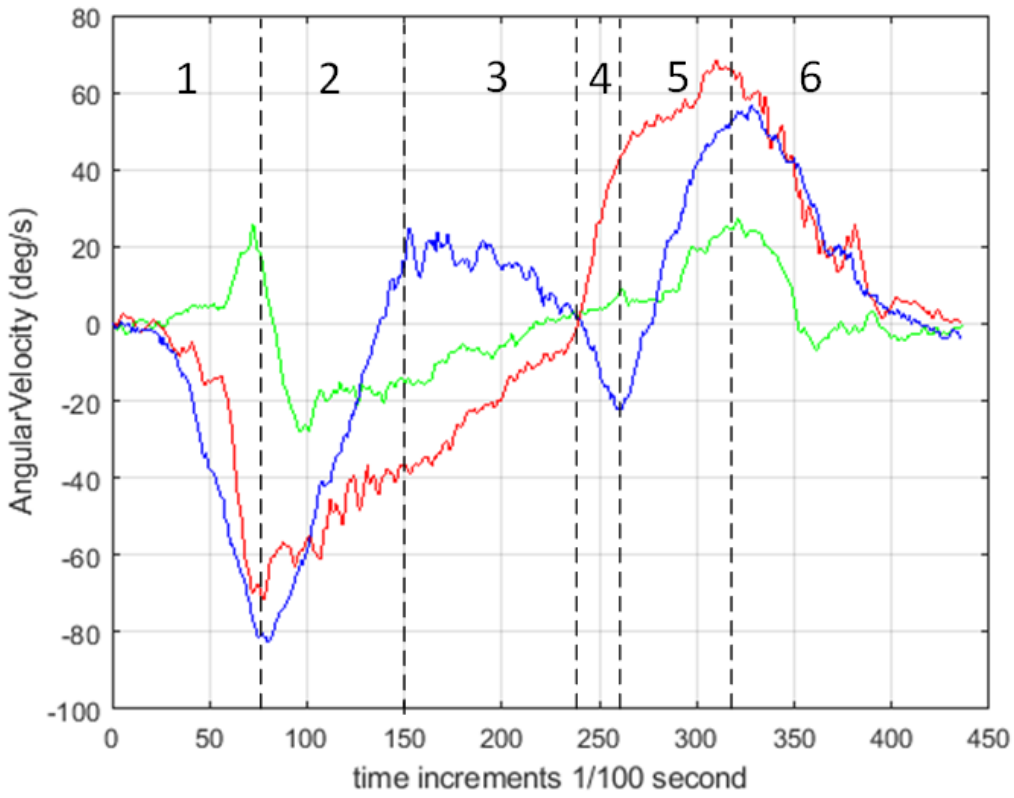

Figure 26. The six discrete stages of back squats in angular velocity for sacrum (blue), thigh (red) and shank (green) in degrees per second.

In stage 1, the thigh increases in the negative angular velocity (downwards), and the sacrum has a similar plot. At the start of stage 2, as forces from the shank come into play, the thigh and sacrum deaccelerate, angular velocity decreases in the negative direction and the gradient becomes positive, thus the plot draws out a "V" shape for the sacrum as of the end of stage 2. At the start of stage 3, the sacrum has positive angular velocity, tilting up to support the back as the thigh reaches the lowest angle at the end of stage 3. At the start of stage 4, the thigh is at the lowest position and begins to ascend, gaining positive angular velocity. At the same time as the thigh is gaining positive angular velocity, the sacrum briefly changes angular direction gaining negative angular velocity downwards for 40 samples at 100Hz, before changing to a positive gradient at the start of stage 5. During the whole of stage 4 the sacrum has increasing negative angular velocity, while the ascending thigh has increasing angular velocity. The negative gradient of the sacrum at this point in time is created by extending the back and pushing down into the floor. This is difficult to achieve for those who have poor back squat technique. It requires physical effort by muscle sets not often used in sedentary life. When performed well, this stage of the cycle gives back squats an impressive dynamic and aesthetic quality. The start of stage 5 occurs where the negative angular velocity of the sacrum changes from increasing to decreasing and the plot changes to a positive gradient. In stage 5 and stage 6, the thigh and sacrum accelerate and deaccelerate as they ascend and return to the start position. The events of the six stages of back squats for angular velocity, as described above with ideal data, are condensed into a truth table (Table 7). Where the percentage of the cycle is calculated by dividing the time period of each stage by the time period of the whole back squat, then multiplying by a hundred.

Table 7. Ideal back squat truth table for angular velocity of sacrum, thigh and shank.

Segment	**Stage 1** Direction / Gradient	**Stage 2** Direction / Gradient	**Stage 3** Direction / Gradient	**Stage 4** Direction / Gradient	**Stage 5** Direction / Gradient	**Stage 6** Direction / Gradient
Sacrum	- / -	- / +	+ / -	- / -	- / +	+ / -
Thigh	- / -	- / +	- / +	+ / +	+ / +	+ / -
Shank	+ / +	+ / -	- / +	+ / +	+ / +	+ / -
% of cycle	18.75%	18.75%	20.00%	10.00%	12.50%	20.00%

From the sequence of gradients pronounced in the plots of angular velocity, a six stage truth table is constructed. This forms the main body of the classifier and appraisal system. Not only is the classifier able to recognise the back squat exercise and count the number of repetitions, but also by calculating the magnitude and duration of the gradients in each of the six stages, give a qualitative appraisal of the performance. An appraisal method considers the gradients and duration from each body segment in each of the six stages to calculate range of motion. With the application of discrete weights based on the technical importance of each gradient in the six-stage cycle, the appraisal is able reflect the technical merit of the back squat. The calculation of a metric for the sign, degree and duration of the gradient of the sacrum in stage 4, could be multiplied several-fold, to ensure that this quality is clearly present in highly appraised back squats.

When the IMMU data is processed to create angular velocity of body segments, the number of gradients increases. For the thigh segment there are two gradients in the negative cycle and two gradients in the positive cycle. The change in gradient direction, negative to positive, at distinct stages of the back squat exercise give the angular velocity data a strong “signature identity”. Changes in angular velocity correspond to key “stages” of body segment kinematics throughout the back squat cycle.

Gradients of angular velocity have the potential to be clearly differentiated by a decision tree algorithm in recognizing kinematic data as back squats exercise and to use slope gradient and duration to qualify the range of motion for sacrum, thigh and shank. Angular velocity gradient slope and duration reduces the burden of the motion capture system to provide highly accurate absolute angle data within the earth frame orientation. If the IMMU is not accurately aligned with the thigh, for example due to the securing elastic strap slipping, then there will be an error in the absolute angle of the body segment. Assuming that the IMMU remains secure for the remaining back squats, this is not critical since while moving out of alignment, the IMMU captures changes in angular velocity. By time duration and angular velocity, the angle through which the thigh traversed is calculated.

When capturing back squat IMMU data with MTx sensors, accelerometer data failed to be recorded. The sensors are no longer supported by their manufacturer, with no possibility of technical support. Running legacy (obsolete) software on the latest Windows 10 operating system is not an ideal situation. The consequences are that there is no accelerometer data for this study, only gyro data. It could be argued that this makes no difference since back squats are performed in a stationary position, where the feet do not move. One possible solution could be to use angle to angle analysis of the thigh and sacrum, so that their positions over time describe a unique cycle for back squats. This would not precisely indicate the start and end of the back squat, since

angles are never exactly the same for any back squat, and IMMU sensors held in place with elastic straps, may slip in alignment with the body segment. Finding the start and end of a back squats with kinematic data is challenging when the time period of a single back squat is unknown. Figure 26 shows the angular velocity of the thigh for a set of six back squats. The second back squat in this series of six, is analysed in the six stages plot of angular velocity in Figure 25.

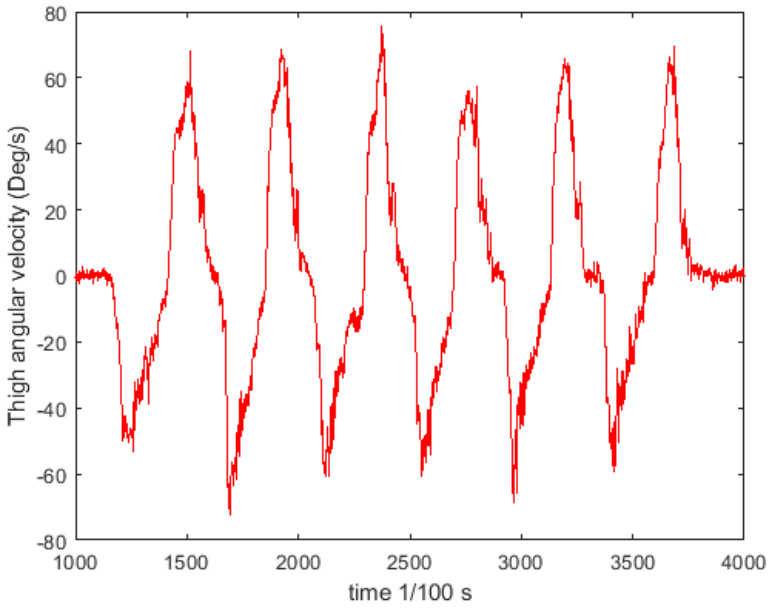

Figure 27. Set of six back squats - thigh angular velocity

The plot of the second derivative, angular acceleration of absolute attitude position of the thigh, calculated using the first central difference method (FCDM). Figure 27 shows a complex sequence of negative and positive acceleration. The plot is a rich combination of many frequencies. There is no uniquely obvious point where the back squat starts and ends. The cyclical nature of the exercise led me to consider a method from gait analysis to find the spectra of a force plate signal: Fourier analysis.

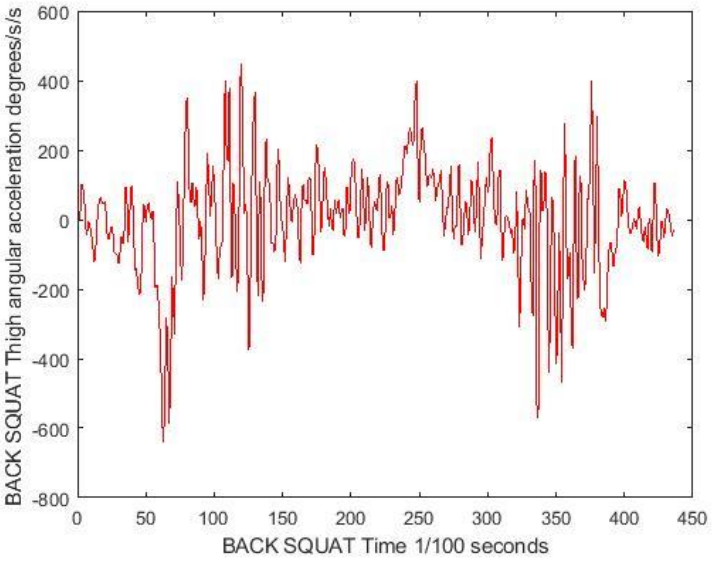

Figure 28. Back squat thigh angular acceleration in degrees per second squared

4.7 Fourier analysis

From literature (Alexander and Jayes, 1980), applied Fourier analysis to human gait, using data of acceleration generated by subjects walking on force plates. The use of Fourier analysis, using the Fast Fourier Transform (FFT) gives detailed analysis of the complex acceleration signals. The FFT transform reveals the individual frequencies that compose the complex signal generated by walking on force plates.

To analyse the back squat absolute position data with the Fourier transform, angular acceleration is calculated using the first central difference method (FCDM). The Fast Fourier Transform (FFT) is based on the Discrete Fourier Transform (DFT), with FFT being preferred since it requires less computation. The results of both transforms are identical, however FFT is more efficient, which is why it is implemented in signal processor hardware and software (Lyons 1997).

In signal processing, signals are either analogue or digital, where analogue is a term to describe a signal that is continuous over time, taking on a continuous range of amplitude values. The term analogue signals could therefore be replaced with continuous signals. The term discrete-time signal is used to describe a signal who independent time variable is quantised so that the amplitude value of the signal is known only at discrete instances in time. Thus, it is not a continuous signal, but represented by a sequence of values taken at a predetermined time interval. In addition to quantising time, a discrete-time signal quantises signal amplitude. A continuous signal may be expressed as a discrete signal by sampling the signal amplitude at some constant time period t_s using an analogue to digital (A/D) converter. The values that are created by an A/D converter form a sequence x(0), x(1), x(2) onwards. The sequence used in discrete systems is abbreviated to x(n) and after processing by a signal processor or software, abbreviated to, y(n). It should be noted that when an analogue signal is quantised only the amplitude is quantised, there is no value recorded for phase, and therefore phase must be "interpreted" from the sequence of amplitudes that form (sampled) discrete signals (Lyons, 1997.)

The problems with sampling discrete signals and phase became a critical issue in this study. The reader may note that the first sentence of this section states that angular acceleration is calculated by the first central difference method (FCDM). Earlier sections describe calculating the angular velocity with the first central difference method. The FCDM method uses values from one sample ahead (in time) and one sample behind, from which the difference in amplitude, is then divided by two sampling periods (double the sampling frequency time period). Prior to using FCDM, this study, out of ignorance used the backwards difference method (BDM), where the difference between the current sample and one sample behind is divided by one sample period (the sampling frequency time period). This calculation results in a phase shift in the angular acceleration, which causes an aliasing error, seen as a signal spike in the FFT frequency domain at approximately 23.8Hz, see Appendix B for the BDM FFT plot.

To prevent issues with aliasing signals outside of the spectra of interest, a low pass digital filter (Figure 28) is placed before the FFT transform, using Matlab Filter Designer in DSP Toolbox version 9.8. The spectra of interest with a back squat cycle is less than one half of a Hertz, since it generally takes longer than two seconds to perform the exercise. Since the back squat is composed of six stages, an allowance is made to permit higher frequencies up to eleven Hertz. Eleven hertz is not a harmonic of the sampling frequency and is selected for the tenth order least-squares Finite Impulse Response (FIR) low pass filter. The corner frequency of 13Hz is where the signal is -3dB, and the 10^{th} order configures a cut-off slope of 200dB per decade (Mathworks, 2019a). The filter has no effect on the in band FFT values.

```
function Hd = FIRLPLS_11hz
%FIRLPLS_11HZ Returns a discrete-time filter object.
% MATLAB Code
% Generated by MATLAB(R) 9.6 and DSP System Toolbox 9.8.
% Generated on: 27-Sep-2019 10:20:09
% FIR least-squares Lowpass filter designed using the FIRLS
function.
% All frequency values are in Hz.

Fs = 100;  % Sampling Frequency

N     = 10;  % Order
Fpass = 11;  % Passband Frequency
Fstop = 13;  % Stopband Frequency
Wpass = 1;   % Passband Weight
Wstop = 1;   % Stopband Weight

% Calculate the coefficients using the FIRLS function.
b  = firls(N, [0 Fpass Fstop Fs/2]/(Fs/2), [1 1 0 0], [Wpass
Wstop]);
Hd = dfilt.dffir(b);
End
```

Figure 29. Matlab script – Tenth order low pass 11Hz finite impulse response filter.

The Fourier transform is a mathematical method to convert a function in the amplitude versus time domain to the amplitude versus frequency domain for non-periodic functions. It does for non-periodic functions what the Fourier series does for periodic functions (van Biezen, 2016.)

A Matlab script to perform Fast Fourier Transform (FFT) on the angular acceleration of the thigh is shown below. When the low pass filter is to be applied before the FFT stage, an additional line of configuration needs to be added with the filter name followed by a

comma then the signal variable, `yf=filter(FIRLPLS_11hz,y);` The output of the filter, yf would then need to be applied to the FFT transform by changing the line `Yaxis = fft (y);` such that the syntax becomes, `Yaxis = fft(yf);` For clarity, only the FFT transform script with no low pass filter applied is shown below.

```
clear all;
close all;
clc
THACC=dlmread('MT_00130431_011-
001_2ndsquat_TH_CDM_AngularAcceleratation.txt');
% Assign delimited read text file, name of THACC.
% Calculate starting point of 2nd squat
% SAcrum THigh and SHank motion data start at sample 19264.
x=THACC(:,1);    % All values column 1, sample #
x=(x-19263);     % 2nd Squat_011-001.txt sample counter starts at
19264
y=THACC(:,8);    % Column 8. Thigh angular acceleration in
degrees/s/s
Fs = 100;        % Sampling frequency 100Hz
L=437;           % Length of signal 437 samples over 4.37 seconds,
                 % duration of the second squat.
Yaxis = fft(y);
% Compute the Fast Fourier Transform (FFT) of the signal,
% angular acceleration of the thigh during back squat.

P2 = abs(Yaxis/L);
% The absolute values or magnitude, negative amplitudes of the
% signal are made positive.
% Plot P1 the single sided spectrum based on P2, and the even
% valued length L.

P1 = P2(1:L/2+1);
% P2 being the double sided amplitude spectrum,
% take one more element than half.
% For odd numbers the result is rounded down

P1(2:end-1) = 2*P1(2:end-1);
% Two sided spectrum has energy split between negative and positive
% frequencies on the frequency axis (X-axis).
% To convert frequency axis to single sided spectrum, discard the
% negative half, and multiple every point on the remaining positive
% side by two, to retain signal power.

f = Fs*(0:(L/2))/L; % Define frequency domain f,
                    % based on Nyquist rate, (50Hz).

plot(f,P1, 'r')     % P1 single sided spectrum in frequency domain.
                    % Plot magnitude P1 against frequency f.
title('Single-Sided Amplitude Spectrum X(t):α thigh angular-accel')
xlabel('f (Hz)')
ylabel('|P1(f)|')
```

Figure 30. Matlab script - Fast Fourier Transform (FFT)

In the Matlab script for Fast Fourier Transform (FFT), (Figure 29), Fs denotes the sampling frequency of 100Hz, L denotes the length of the signal which in this case is 437 samples. By default, the Matlab FFT uses windowing to reduce leakage, which although not listed in the FFT script, the default utilises a rectangular window function

(Mathworks, 2019b). Leakage occurs when a non-infinite signal stops abruptly, creating high frequencies. Changing the shape of the window function, where values of the window coefficient are at a minimum at the start and end of the data sample, is a method to reduce leakage, which results in additional frequencies being revealed. For example using a Hann window where the vectors produced by the FFT transform are multiplied by the Hann window coefficients.

The output of the FFT displays the amplitude of frequencies over the Nyquist rate of fifty Hertz, which is half of the sampling rate. The output is single-sided, which means that the negative frequencies, those below the Direct Current (DC) value of zero Hertz are discarded. The FFT transform doubles the frequency amplitude on the single sided plot to compensate for the loss of power. Because the negative side of the plot is discarded, half of the samples are lost, this is by definition of the Nyquist Shannon criterion. Also, the number of bins is halved. There remain $n/2 + 1$ bins, where n is the number of samples. In this transform with 437 samples, there remain 219 bins in the single sided output. A bin is a range where frequencies collect, each bin counts the occurrence of frequencies within its range. The Nyquist frequency divided by the number of bins, determines the frequency resolution of the FFT transform (Lyons 1997). In this case 50Hz divided by 219 bins results in a resolution of 0.23Hz.

5. Findings

5.1 Back squat exercise classifier and appraisal method

After plotting data of angular velocity from a subject with good technique, the direction and gradients of the plots described a clear cyclic pattern of the exercise. From the visible cycle pattern a six stage truth table was constructed. The efficacy of the truth table was tested with kinematic data from a subject with poor back squat technique and limited ROM.

The motion capture system Xsens MTx was configured to sample at only 50Hz, 0.02 seconds between samples, to prove that the lower sampling rate is sufficient to count and appraise the performance quality of back squats. The athlete who performed the back squat is less experienced at back squat technique than the first athlete. The second athlete is 15 centimetres taller at 1.80m, fifty-two years of age, male, 80kg with tight hamstrings. The subject had a history of an Achilles injury and a lower back which is rather inflexible due to a teenage schoolboy trauma where a complete idiot pulled away a chair injuring his coccyx. The classifier test with the second athlete with reduced range of motion, demonstrated that the six stage truth table is able to recognise and also appraise back squats from athletes with limited ROM as well as experienced fully fit athletes. The six stage truth table was able to recognize and appraise the quality of the back squat technique as poor with a sampling frequency of fifty Hertz (Figure 30).

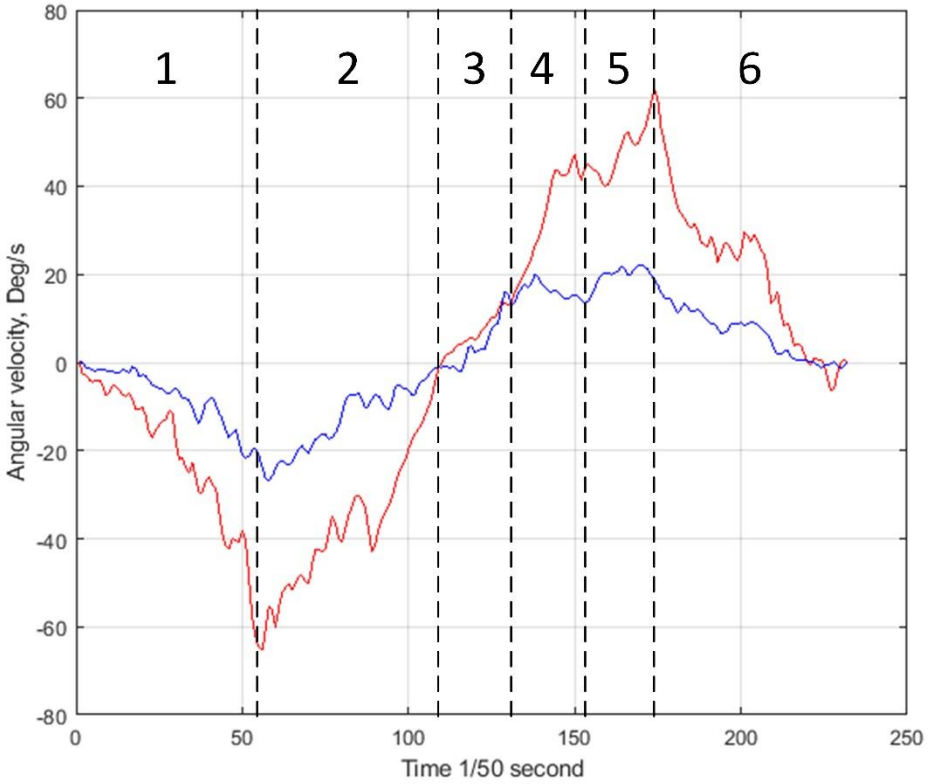

Figure 31. Poor technique shown with six discrete stages of back squat in angular velocity for sacrum (blue), and thigh (red).

Unfortunately, the IMMU on the shank failed to record data, however this did not prevent recognition and appraisal of the back squat via the truth table by sacrum and thigh data alone. Although the time periods of the exercises were similar, 4.6 compared to 4.2 seconds, the gradients in stage 1 and 2 are not as steep compared to good technique (Figure 25). The proportions of the six stages had changed dramatically, stages 1 and 2 last 2.2 seconds, whereas with good technique they lasted just 1.2 seconds. Conversely, stage 3 was much shorter compared to good technique, lasting only 0.5 seconds against 0.8 seconds. This short time period for stage 3 was due to the sacrum absolute position rotating through only 20 degrees, as compared to fifty degrees with good technique. Also at the start of stage 3, the thigh was already moving upwards, whereas with the athlete with good technique the thigh continued in the descent phase until the end of stage 3. In stage 4, where the sacrum rotates down, the gradient of angular velocity was approximately only a quarter of that with good technique. Stages 5 and 6 last the same as with good technique, but the profile of the change in gradient was very different, the poor technique plot accelerating at the stage 5 to 6 boundary. Whereas with good technique the acceleration was at the start of stage 5 and de-acceleration closer to the end of stage 6. Unlike the poor back squat technique with a spiked profile, the good back squat technique had a more rounded and full profile in stages 5 and 6, which when performed demonstrated more control and a richer smoother dynamic.

Table 8. Poor back squat truth table for angular velocity of sacrum and thigh.

Segment	**Stage 1** Direction / Gradient	**Stage 2** Direction / Gradient	**Stage 3** Direction / Gradient	**Stage 4** Direction / Gradient	**Stage 5** Direction / Gradient	**Stage 6** Direction / Gradient
Sacrum	- / -	- / +	+ / +	+ / -	+ / +	+ / -
Thigh	- / -	- / +	+ / +	+ / +	+ / +	+ / -
% of cycle	23.40%	25.53%	8.51%	10.63%	8.51%	23.40%

From the angular velocity truth table for the poor back squat (Table 8), stage 3 for the sacrum had a positive direction and gradient. Whereas in the truth table for a good back squat (Table 7), the sacrum had a positive sign with a negative gradient. The thigh in stage 3 of the poor back squat had a positive direction and gradient. This was not the case for a good back squat (Table 7) where the thigh had a downwards direction and negative gradient. In stage 4 the poor back squat sacrum had positive (upwards) direction and a negative gradient, as opposed to the good back squat (Table 7) which had a negative direction (downwards) and a negative gradient. Thus, by comparing the six stages of the poor back squat truth table to the good back squat truth table, there were three stages of the truth table indicating that the second back squat was of poor quality. The kinematic data from the novice athlete data with a sampling rate of 50Hz, successfully validated the six-stage truth table appraisal method.

5.2 Back squat time duration

One limitation of utilizing the truth table in a practical algorithm was finding the start of the exercise cycle. Using Fast Fourier Transform (FFT), with angular acceleration of the thigh, the time duration of the back squat exercise was resolved. The FFT transform was able to give a time period based on a single cycle, or on several cycles by giving an average. The FFT transform was unable to give the individual time periods from a sample period that lasts several cycles due to the limits of frequency resolution which is determined by the number of samples and the Nyquist-Shannon criterion of the sampling frequency.

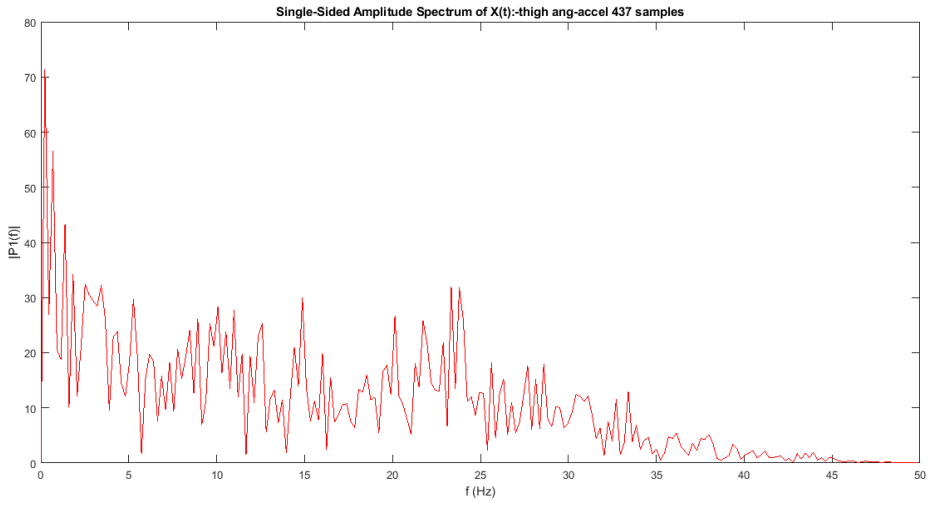

Figure 32. Back squat FFT, amplitude against frequency.

To reveal the frequencies with the greatest amplitude required the use of the plot zoom function. The primary frequency of the back squat exercise is revealed in the FFT plot at 0.2288 Hertz, the inverse of which of 4.37 seconds. An accurate result that validated the method for the 2nd back squat time period.

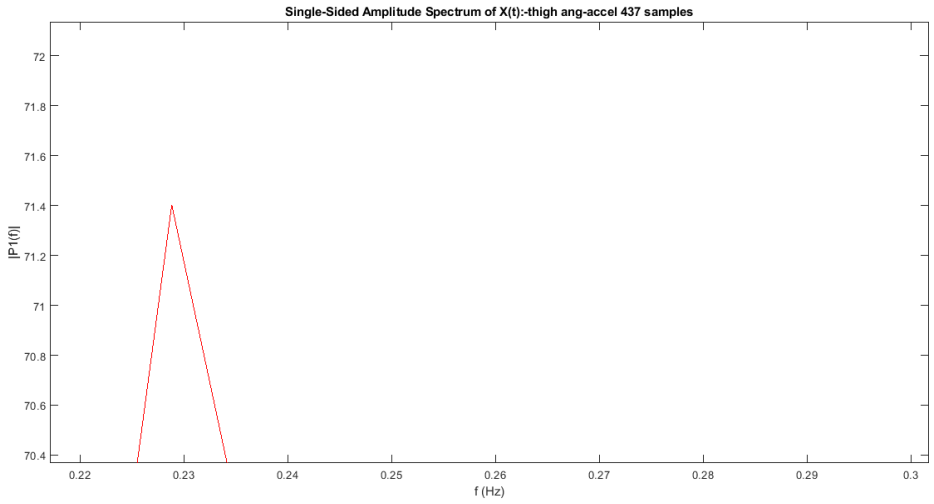

Figure 33. Back squat FFT showing the greatest amplitude at 0.2288Hz.

The second greatest amplitude occurred at 0.6865Hz, the inverse of which was 1.45 seconds. This was approximately the time taken in for stages 1 and 2 to complete. It also matches the time for stages 4, 5 and 6 to complete. The third largest magnitude was found at 1.373Hz the inverse of which is 0.728 seconds. The time period of 0.72 seconds was found in the plot of angular velocity to be a close match for four stages, stage 1, stage 2, stage 5 and stage 6. which all individually matched the 0.72 seconds time period.

The gradient of angular velocity is the sign and magnitude of angular velocity, which gave more detail than the spectra found by Fourier transform. There was also the issue of frequency resolution with Fourier. The FFT resolution is given by the Nyquist frequency divided by the number of bins, in this case 50 divided by 219 bins equals 0.228 Hz resolution. Each bin has an accuracy of plus or minus 0.114Hz. The resolution of the bin range was for signals with a time period of 2.9 to 8.7 seconds. Since the set of six squats have time periods of 4.07 to 4.62 seconds, the FFT transform with a sampling rate of 100Hz was unable to separate each squat as a separate frequency. To increase the frequency resolution of the FFT transform, the sampling frequency must be increased or the duration of the signal prolonged, repeated multiple times (Lyons, 1997).

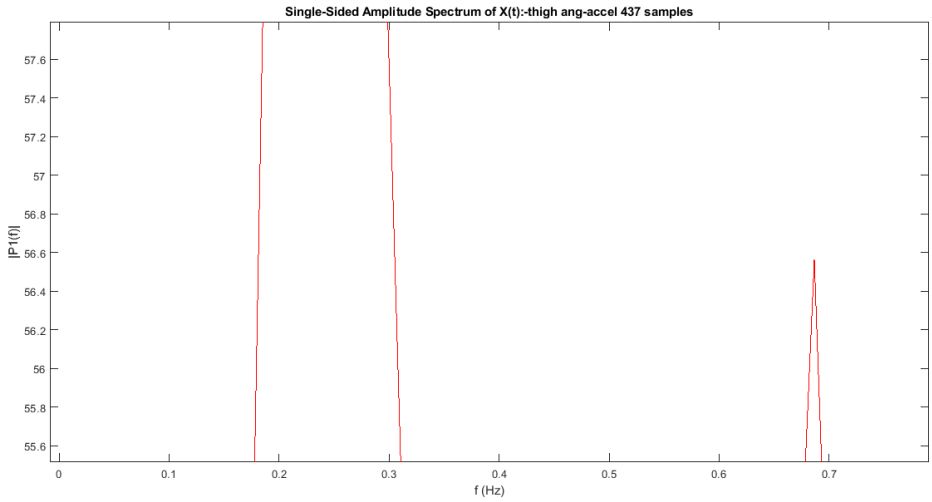

Figure 34. Back squat FFT showing amplitude of the second greatest amplitude at 0.6865Hz.

Sampling rate is a key component of Fourier analysis since it is a factor in the frequency resolution of the transform. Although at 100Hz sampling the FFT transform is unable to separate back squats with a time period of between 4.07 and 4.62 seconds, this is useful information since due to their cyclic nature people usually perform back squats with a steady rhythm. Knowing the length of a set of back squats time period within ten percent would be better than having no value at all before entering a decision tree algorithm, since the first task of a classifier is the segmentation of the data (O'Reilly et al., 2017). Knowing the minimum time duration of the sampled data to process with the decision tree, allows the sample stream to be broken up into segments of a suitable length. A contrary argument could be that FFT is too processor intensive to justify use on mobile platforms. In an attempt to address this issue, angular acceleration data from the poorly performed back squat sampled at fifty Hertz angular is analysed.

From the FFT transform plot (Figure 34), a sampling frequency of 50Hz was utilised to measure the time period of a single squat or several back squats performed with an even rhythm. Kinematic data for back squat exercise at fifty Hertz sampling frequency gave comparable results when back squats of four seconds or more duration were analysed, both by angular velocity with the six-stage truth table and by angular acceleration of the thigh with the FFT transform

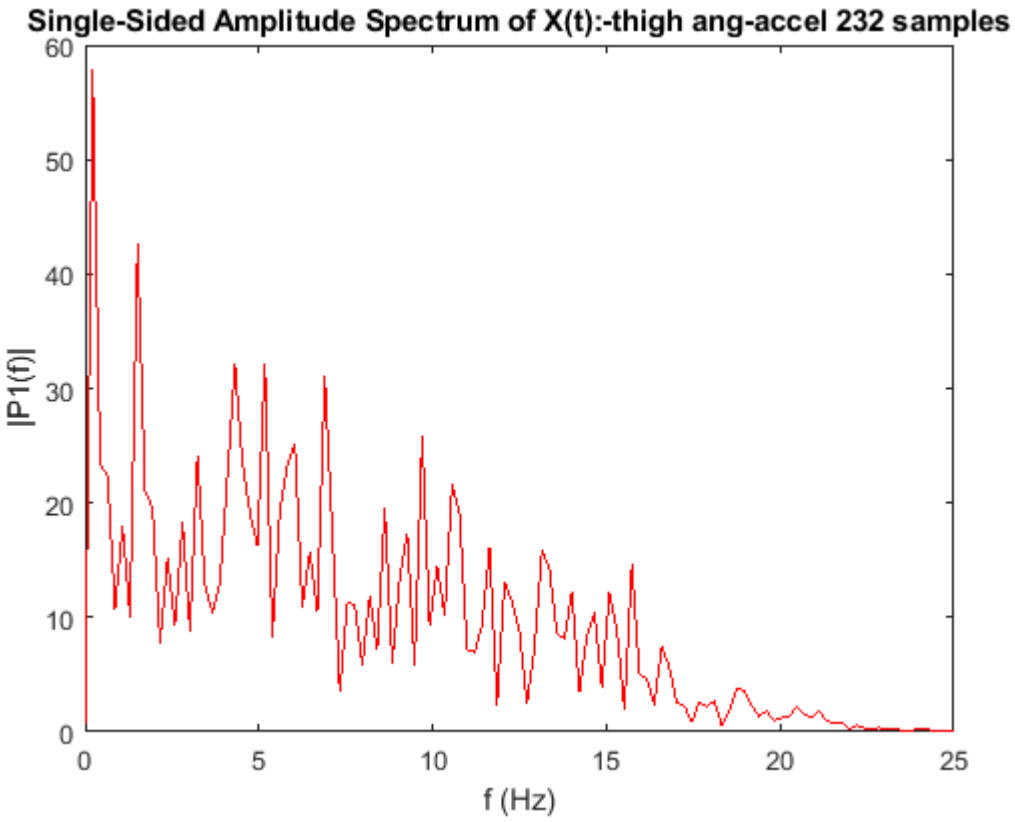

Figure 35. FFT of back squat sampled at 50Hz.

6. Discussion

6.1 Main findings

Research for developing a system classifier to recognize and appraise back squat exercise, based on IMMU kinematic data from sacrum, thigh and shank, found that angular velocity is suitable for processing with a six-stage truth table. The use of fast Fourier transform (FFT) with angular acceleration is proven to be suitable for detecting the time period of a back squat or a sequence of several evenly paced back squats. Time period being useful in determining data segmentation size by the classifier. Angular velocity of sacrum and thigh from back squats performed with good and poor technique are both successfully recognized and appraised with the six-stage truth table. The artefact in this DSR study, a back squat classifier with appraisal features constructed from Matlab scripts, utilising a six-stage truth table and FFT methods are validated with kinematic data sampled at one hundred Hertz and also at fifty Hertz sampling frequency.

6.2 What does this research add to the existing body of knowledge?

The FFT transform in gait analysis and human movement has been used for decades (Alexander and Jayes, 1980). The use of FFT as a method in human activity classification algorithms by smartphone on-board accelerometers is documented as a successful approach by Spinsante et al., (2016). In this study, the ability to develop a classifier to count and appraise back squats is considered a condition for achieving a practical system that would be of use to general musculoskeletal physiotherapy. The use of FFT frequency domain analysis proved to be a suitable method to gauge exercise repetition time, as a measure for segmenting data before activity feature extraction. In the absence of accelerometer data, gyroscope data is the single source of activity recognition. The use of angular velocity to analyse powerlifting squats in three descent and three ascent phases is described in biomechanics (Escamilla et al. 2001b). The artefact in this study, a classifier constructed from Matlab scripts is validated to be able to recognise and appraise back squat kinematic data from wearable gyroscope sensors. No accelerometer data is used by the classifier in appraising back squats.

Methods to apply kinematic data from wearable IMMU sensors during squat exercise has been studied previously. From literature (Rungsawasdisap et al., 2018) implemented hidden Markov methods (HMM) with Baum-Welch machine learning method to kinematic data from ten IMMUs sampling at a frequency of 69Hz. Their system aimed to help users correct their squats. Movement recognition being achieved through a matrix of observation probabilities and probability distributions proved to be over 80% accurate in tests with standard squats. However, the system was considered difficult to apply in a practical situation due to issues of magnetic interference with IMMU sensors. Their results are comparable with this study where it is found that subjects are required to exercise more than three meters away from steel framed gym training machines to avoid magnetic interference with IMMUs.

A study by Zhou et al. (2017), implemented an exercise recognition system with textile resistive pressure mapping systems. As with this study, their system was capable of operating with a sampling frequency of 50Hz. For the exercise recognition algorithms, decision-tree and dynamic time warping methods were utilised to produce a confusion matrix, the reliability of the recognition algorithms varied between subjects.

Although decision tree algorithms and data segmentation techniques are suitable to detect back squats with kinematic data, the use of FFT, due to short run-time make it an option when analysing a cyclical exercise such as back squats. The study proved that angular acceleration in the sagittal plane of the thigh is suitable for FFT analysis revealing the frequency of the back squat cycle.

Escamilla et al. (2001) performed biomechanical analysis of power-lifting squats in three descent and three ascent phases, using angular displacement and angular velocity. This study developed a six stage truth table to recognise and appraise back squats from angular velocity of the sacrum and thigh. The six stage truth table is developed using kinematic data from a single athlete with good technique. The truth table is tested with data from a second athlete with poor technique. The test results of the appraisal confirm the poor back squat technique of the novice athlete. The back squat technique being classified as poor from the results of the fourth stage of the framework. The appraisal ability of the truth table is tested with just one subject due to wearable IMMU availability and time constraints.

6.3 Methodological considerations

The study employs a design science research framework. The proposed system developed from background review is tested for relevance with ideal data captured in laboratory conditions. The ideal data is used to demonstrate the system functions to practicing physiotherapists to gain the relevance of the system in practice. The interviews are unstructured and conducted in an informal manner following a system presentation.

The physiotherapists interviewed in the relevance cycle of the study are from a small geographic distribution and their mother tongue is not the same as that of the interviewer. Those that consent to the interview do so through a network of personal contacts. The study is not able to prove that the sample is representative of physiotherapists in the profession as a whole. Only four interviews are conducted, too small to form the basis of any meaningful statistical analysis.

When processing kinematic data from back squats performed in laboratory conditions by an athlete with good technique, calculations made for angular velocity and angular acceleration are in the first instance made with a flawed method. The problems experienced with the backwards difference method resulted in new DSR design iterations to resolve the issue. The backwards difference method is used in ignorance rather than by a method described from biomechanics literature, the first central difference method (FCDM). The consequence of this failing in the background review is aliasing in the FFT transform (Appendix B). The aliasing problem being resolved by the adoption of the first central difference method.

6.3.1 Reliability

Kinematic data collected from the thigh in the transverse and frontal planes appears unreliable. Muscle bulge causing IMMUs on the thigh and shank to tilt out of true alignment in these two planes. For this reason, measurement of knee valgus and varus was considered outside of the scope of study.

The physiotherapists that consented to the interview are clearly passionate about their profession and welcomed research into the use of new technology. Therefore, they may have been biased in their views on the use of technology in physiotherapy. There was no financial gain or any other incentive for giving the interview. I consider that all of the physiotherapists in the study are open, honest, and completely professional in their appraisal.

All of the signal processing is conducted within the Matlab environment, none of the methods are embedded or tested within a real-time target system.

6.3.2 Limitations

Although the back-squat analysis truth table is able to appraise exercise with a sampling rate of fifty Hz, the FFT method to find the cycle period has a frequency resolution limited by the Nyquist rate and the number of samples processed. In the case of one hundred Hertz sampling frequency, the resolution of the bin range included signals with a time period of 2.9 to 8.7 seconds. This prevents the individual time measurement of each back squat from a set of repetitions. However, the average time period from a set of repetitions is sufficient for the purposes of segmenting data for a classifier window.

The back squat classifier system worked with kinematic data only. From literature, no skeletal body modeling or anatomical muscle models were considered for musculoskeletal loading (Schellenberg et al., 2015). Muscle bulge due to muscle contractions of the femur made measurements of knee valgus and varus highly inaccurate. This study agrees with Rungsawasdisap et al., (2018) in that magnetic interference with IMMUs make a practical system challenging.

6.4 Future directions

The two areas of physiotherapy that received the most positive feedback are, teaching squat technique to patients who have never performed the exercise, and sportsmen and women recovering from injury, who are naturally motivated by numbers. Any further development of the system would do well to keep sports science and sport coaching in mind. Once a practical system is functioning, a technical action research (TAR) study could be undertaken to validate the artefact in the field of general musculoskeletal physiotherapy.

The one unexpected finding of the study is a feature request made by all students of physiotherapy and all physiotherapists sampled with the exception of post-operative physiotherapists; the feature request being a Bluetooth goniometer app. A Bluetooth wireless goniometer that measured knee angle with wearable thigh and shank sensors. A Bluetooth goniometer to measure knee angle may be worth further research, developed either as a separate app or an inclusive feature.

Although the FFT transform in Matlab successfully resolves the exercise time period, the time period provided is not tested with a sliding window feature extraction algorithm. Further development of the classifier would give a more detailed appraisal of the benefits of running FFT to acquire back squat time period. This study ran truth table tests on a single subject. Further work would require the testing of the classifier truth table on a much larger sample size. Once a larger sample size is established, statistical analysis and machine learning could be based on the results of classifier back squat truth table.

Problems with muscle bulge when attempting to measure knee valgus or varus require further study to find positions on the thigh and shank which could defeat this problem. For example on the flat surface of the lower medial surface of the tibia.

7. Conclusions

From the work conducted on kinematic data in the Matlab environment, angular velocity of the sacrum and thigh in the sagittal plane is well suited for recognizing and appraising back squats by means of a six-stage truth table. Thigh angular acceleration in the sagittal plane when processed by FFT transform is found to give the time period for a back squat exercise. The time period is considered useful when segmenting kinematic data before the classifier system commences feature extraction. By the combination of both methods, sacrum and thigh angular velocity six stage truth table, and FFT transform of angular acceleration, the scripts created in Matlab were tested and proven able to classify and appraise back squat exercise.

References

Alexander, R. M., & Jayes, A. S. (1980). Fourier analysis of forces exerted in walking and running. Journal of biomechanics, 13(4), 383-390.

Allahbakhshi, H., Hinrichs, T., Huang, H., & Weibel, R. (2019). The Key Factors in Physical Activity Type Detection Using Real-Life Data: A Systematic Review. Frontiers in physiology, 10, 75. doi:10.3389/fphys.2019.00075

Atkins, Clare, and Gail Louw. "Reclaiming knowledge: a case for evidence based information systems." ECIS 2000 Proceedings (2000): 28.

Chang, K. H., Chen, M. Y., & Canny, J. (2007, September). Tracking free-weight exercises. In International Conference on Ubiquitous Computing (pp. 19-37). Springer, Berlin, Heidelberg.

Cheng, H. T., Sun, F. T., Griss, M., Davis, P., Li, J., & You, D. (2013, June). Nuactiv: Recognizing unseen new activities using semantic attribute-based learning. In Proceeding of the 11th annual international conference on Mobile systems, applications, and services (pp. 361-374). ACM.

Coffey, A., & Atkinson, P. (1996). Making sense of qualitative data: complementary research strategies. Sage Publications, Inc.

Cotter, J. A., Chaudhari, A. M., Jamison, S. T., & Devor, S. T. (2013). Knee joint kinetics in relation to commonly prescribed squat loads and depths. Journal of strength and conditioning research/National Strength & Conditioning Association, 27(7), 1765.

Denning, P. J. (1997). A new social contract for research. Communications of the ACM, 40(2), 132-134.

De Vries, S. I., Garre, F. G., Engbers, L. H., Hildebrandt, V. H., & Van Buuren, S. T. E. F. (2011). Evaluation of neural networks to identify types of activity using accelerometers. Med Sci Sports Exerc, 43(1), 101-7.

Diebel, J. (2006). Representing attitude: Euler angles, unit quaternions, and rotation vectors. Matrix, 58(15-16), 1-35.

Ding, H., Shangguan, L., Yang, Z., Han, J., Zhou, Z., Yang, P., ... & Zhao, J. (2015, November). Femo: A platform for free-weight exercise monitoring with rfids. In Proceedings of the 13th ACM Conference on Embedded Networked Sensor Systems (pp. 141-154). ACM.

Escamilla, R. F. (2001a). Knee biomechanics of the dynamic squat exercise. Medicine & Science in Sports & Exercise, 33(1), 127-141.

Escamilla, R. F., Fleisig, G. S., Lowry, T. M., Barrentine, S. W., & Andrews, J. R. (2001b). A three-dimensional biomechanical analysis of the squat during varying stance widths. Medicine & Science in Sports & Exercise, 33(6), 984-998.

Euler, L. (1776). Formulae generales pro translatione quacunque corporum rigidorum. Novi Commentarii academiae scientiarum Petropolitanae, 189-207.

Fry, A. C., Smith, J. C., & Schilling, B. K. (2003). Effect of knee position on hip and knee torques during the barbell squat. The Journal of Strength & Conditioning Research, 17(4), 629-633.

Google Developers (2019). Google APIs for Android Reference ActivityRecognitionClient. Retrieved November 5, 2019, from https://developers.google.com/android/reference/com/google/android/gms/location/ActivityRecognitionClient.html#inherited-method-summary.

Gresham, G., Hendifar, A. E., Spiegel, B., Neeman, E., Tuli, R., Rimel, B. J., ... & Shinde, A. M. (2018). Wearable activity monitors to assess performance status and predict clinical outcomes in advanced cancer patients. npj Digital Medicine, 1(1), 27.

Gyllensten, I. C., & Bonomi, A. G. (2011). Identifying types of physical activity with a single accelerometer: evaluating laboratory-trained algorithms in daily life. IEEE transactions on biomedical engineering, 58(9), 2656-2663.

Hamill, J., & Knutzen, K. M. (2006). Biomechanical basis of human movement. Lippincott Williams & Wilkins.

Hevner, A., March, S. T., Park, J., & Ram, S. (2004). Design science research in information systems. MIS quarterly, 28(1), 75-105.

Hevner, A. R. (2007). A three cycle view of design science research. Scandinavian journal of information systems, 19(2), 4.

Horschig, A. D., Neff, T. E., & Serrano, A. J. (2014). UTILIZATION OF AUTOREGULATORY PROGRESSIVE RESISTANCE EXERCISE IN TRANSITIONAL REHABILITATION PERIODIZATION OF A HIGH SCHOOL FOOTBALL- PLAYER FOLLOWING ANTERIOR CRUCIATE LIGAMENT RECONSTRUCTION: A CASE REPORT. International journal of sports physical therapy, 9(5), 691.

KAHLE, L. (1986). Text of Human Anatomy. Nervus System and sensory organs. Thieme. New York. Pp, 104-111.

Kato, A., Matsumoto, Y., Kobayashi, Y., Sugano, S., & Fujie, M. G. (2015, December). Estimating a joint angle by means of muscle bulge movement along longitudinal direction of the forearm. In 2015 IEEE International Conference on Robotics and Biomimetics (ROBIO) (pp. 614-619). IEEE.

Klein, H. K., & Myers, M. D. (1999). A set of principles for conducting and evaluating interpretive field studies in information systems. MIS quarterly, 23(1), 67-94.

Kok, M., Hol, J. D., Schön, T. B., Gustafsson, F., & Luinge, H. (2012, July). Calibration of a magnetometer in combination with inertial sensors. In 2012 15th International Conference on Information Fusion (pp. 787-793). IEEE.

Leardini, A., Chiari, L., Della Croce, U., & Cappozzo, A. (2005). Human movement analysis using stereophotogrammetry: Part 3. Soft tissue artifact assessment and compensation. Gait & posture, 21(2), 212-225.

Li, J., Zhou, Y., Lu, Y., Zhou, G., Wang, L., & Zheng, Y. P. (2013). The sensitive and efficient detection of quadriceps muscle thickness changes in cross-sectional plane using ultrasonography: a feasibility investigation. IEEE Journal of Biomedical and Health Informatics, 18(2), 628-635.

Lorenzetti, S., Gülay, T., Stoop, M., List, R., Gerber, H., Schellenberg, F., & Stüssi, E. (2012). Comparison of the angles and corresponding moments in the knee and hip during restricted and unrestricted squats. The Journal of Strength & Conditioning Research, 26(10), 2829-2836.

Lorenzetti, S., Ostermann, M., Zeidler, F., Zimmer, P., Jentsch, L., List, R., ... & Schellenberg, F. (2018). How to squat? Effects of various stance widths, foot placement angles and level of experience on knee, hip and trunk motion and loading. BMC Sports Science, Medicine and Rehabilitation, 10(1), 14.

Lyons, R. (1997). Understanding digital signal processing 1 rd.

Mathworks, Inc. (2019a). Designing Low Pass FIR Filters. Retrieved November 9, 2019 from https://se.mathworks.com/help/dsp/examples/designing-low-pass-fir-filters.html?searchHighlight=cutofffrequency&s_tid=doc_srchtitle

Mathworks, Inc. (2019b). MathWorks Conversations and the FFT. Retreived November 9, 2019 from https://blogs.mathworks.com/simulink/2009/01/30/mathworks-conversations-and-the-fft/

Maxwell, J. A. (2008). Designing a qualitative study. The SAGE handbook of applied social research methods, 2, 214-253.

McCarthy, M., & Grey, M. (2015). Motion sensor use for physical activity data: Methodological considerations. Nursing research, 64(4), 320.

Mokaya, F., Lucas, R., Noh, H. Y., & Zhang, P. (2015, September). Myovibe: Vibration based wearable muscle activation detection in high mobility exercises. In Proceedings of the 2015 ACM International Joint Conference on Pervasive and Ubiquitous Computing (pp. 27-38). ACM.

Mourcou, Q., Fleury, A., Franco, C., Klopcic, F., & Vuillerme, N. (2015). Performance evaluation of smartphone inertial sensors measurement for range of motion. Sensors, 15(9), 23168-23187.

Myer, G. D., Kushner, A. M., Brent, J. L., Schoenfeld, B. J., Hugentobler, J., Lloyd, R. S., ... & McGill, S. M. (2014). The back squat: A proposed assessment of functional deficits and technical factors that limit performance. Strength and conditioning journal, 36(6), 4.

O'Reilly, M. A., Johnston, W., Buckley, C., Whelan, D., & Caulfield, B. (2017, May). The influence of feature selection methods on exercise classification with inertial measurement units. In 2017 IEEE 14th International Conference on Wearable and Implantable Body Sensor Networks (BSN) (pp. 193-196). IEEE.

Patton, M. Q. (2002). Qualitative research and evaluation methods. Thousand Oaks. Cal.: Sage Publications.

Pérez, R., Costa, Ú., Torrent, M., Solana, J., Opisso, E., Cáceres, C., ... & Gómez, E. J. (2010). Upper limb portable motion analysis system based on inertial technology for neurorehabilitation purposes. Sensors, 10(12), 10733-10751

Peterson, S. (2018). Telerehabilitation booster sessions and remote patient monitoring in the management of chronic low back pain: A case series. Physiotherapy theory and practice, 34(5), 393-402.

Physiofile Oy. (2019). Free Exercise Library. Retrieved November 05, 2019, from https://physiofile.fi/index.php

Physiotools Oy. (2019). Home Exercise Programs. Retrieved November 05, 2019, from https://www.physiotools.com/

Picha, K. J., & Howell, D. M. (2018). A model to increase rehabilitation adherence to home exercise programs in patients with varying levels of self- efficacy. Musculoskeletal Care, 16(1), 233-237.

Roetenberg, D., Luinge, H., & Slycke, P. (2009). Xsens MVN: Full 6DOF human motion tracking using miniature inertial sensors. Xsens Motion Technologies BV, Tech. Rep, 1.

Rungsawasdisap, N., Yimit, A., Lu, X., & Hagihara, Y. (2018, January). Squat movement recognition using hidden Markov models. In 2018 International Workshop on Advanced Image Technology (IWAIT) (pp. 1-4). IEEE.

Sabatini, A. M. (2011). Estimating three-dimensional orientation of human body parts by inertial/magnetic sensing. Sensors, 11(2), 1489-1525.

Scheepers, F., Parent, R. E., Carlson, W. E., & May, S. F. (1997, August). Anatomy-based modeling of the human musculature. In Proceedings of the 24th annual conference on Computer graphics and interactive techniques (pp. 163-172). ACM Press/Addison-Wesley Publishing Co..

Schellenberg, F., Oberhofer, K., Taylor, W. R., & Lorenzetti, S. (2015). Review of modelling techniques for in vivo muscle force estimation in the lower extremities during strength training. Computational and mathematical methods in medicine, 2015.

Shen, C., Ho, B. J., & Srivastava, M. (2018). Milift: Efficient smartwatch-based workout tracking using automatic segmentation. IEEE Transactions on Mobile Computing, 17(7), 1609-1622.

Shoaib, M., Bosch, S., Incel, O., Scholten, H., & Havinga, P. (2014). Fusion of smartphone motion sensors for physical activity recognition. Sensors, 14(6), 10146-10176.

Simon, H. (1996). The Sciences of the Artificial 3 rd ed MIT Press. Cambridge, MA.

Singla, P., Mortari, D., & Junkins, J. L. (2004). How to avoid singularity when using Euler angles. Advances in the Astronautical Sciences, 119, 1409-1426.

Spinsante, S., Angelici, A., Lundström, J., Espinilla, M., Cleland, I., & Nugent, C. (2016). A mobile application for easy design and testing of algorithms to monitor physical activity in the workplace. Mobile Information Systems, 2016.

Texas Instruments. (2015). Multi-Standard CC2650 SensorTag Design Guide. Retrieved June 15, 2019, from http://www.ti.com/lit/ug/tidu862/tidu862.pdf

Tognetti, A., Lorussi, F., Carbonaro, N., & De Rossi, D. (2015). Wearable goniometer and accelerometer sensory fusion for knee joint angle measurement in daily life. Sensors, 15(11), 28435-28455.

Tsichritzis, D. (1998). The Dynamics of Innovation in Beyond Calculation: The Next Fifty Years of Computing, PJ Denning and RM Metcalfe.

van Biezen, M. 2016. Electrical Engineering Ch 19: Fourier Transform (1 of 45) What is a Fourier Transform? Retrieved November 3, 2019, from https://www.youtube.com/watch?v=7hSMtRdHutY&list=PLX2gX-ftPVXVTT3qpUeHVxbmJx9D1vGhC&index=1

Wang, Wei-zhong, et al. "Analysis of filtering methods for 3D acceleration signals in body sensor network." International Symposium on Bioelectronics and Bioinformations 2011. IEEE, 2011.

Warren, G. W. (1989). Classical ballet technique. University of South Florida Press.

Wieringa, R. J. (2014). Design science methodology for information systems and software engineering. Springer.

Xsens Technologies B.V. (2006) Mti and MTx User Manual and Technical Documentation Revision G. Retrieved June 15, 2019, from http://wiki.icub.org/images/8/82/XsensMtx.pdf

Xu, J. Y., Sun, Y., Wang, Z., Kaiser, W. J., & Pottie, G. J. (2011, October). Context guided and personalized activity classification system. In Proceedings of the 2nd Conference on Wireless Health (p. 12). ACM.

Zebin, T. (2018). Wearable inertial multi-sensor system for physical activity analysis and classification with machine learning algorithms (Doctoral dissertation, University of Manchester).

Zhang, R., & Reindl, L. M. (2011, February). Pedestrian motion based inertial sensor fusion by a modified complementary separate-bias Kalman filter. In 2011 IEEE Sensors Applications Symposium (pp. 209-213). IEEE.

Zhang, S., McCullagh, P., Nugent, C., & Zheng, H. (2010, July). Activity monitoring using a smart phone's accelerometer with hierarchical classification. In 2010 Sixth International Conference on Intelligent Environments (pp. 158-163). IEEE.

Zhang, Y., & Wildemuth, B. M. (2009). Unstructured interviews. Applications of social research methods to questions in information and library science, 222-231.

Zhou, B., Sundholm, M., Cheng, J., Cruz, H., & Lukowicz, P. (2017). Measuring muscle activities during gym exercises with textile pressure mapping sensors. Pervasive and Mobile Computing, 38, 331-345.

Zhou, H., & Hu, H. (2009). Reducing drifts in the inertial measurements of wrist and elbow positions. IEEE Transactions on Instrumentation and Measurement, 59(3), 575-585.

Appendix A. Student feedback of the system presentation via Padlet

In the second phase of the study, first year physiotherapy student gave their feedback via Padlet to the proposed system presentation.

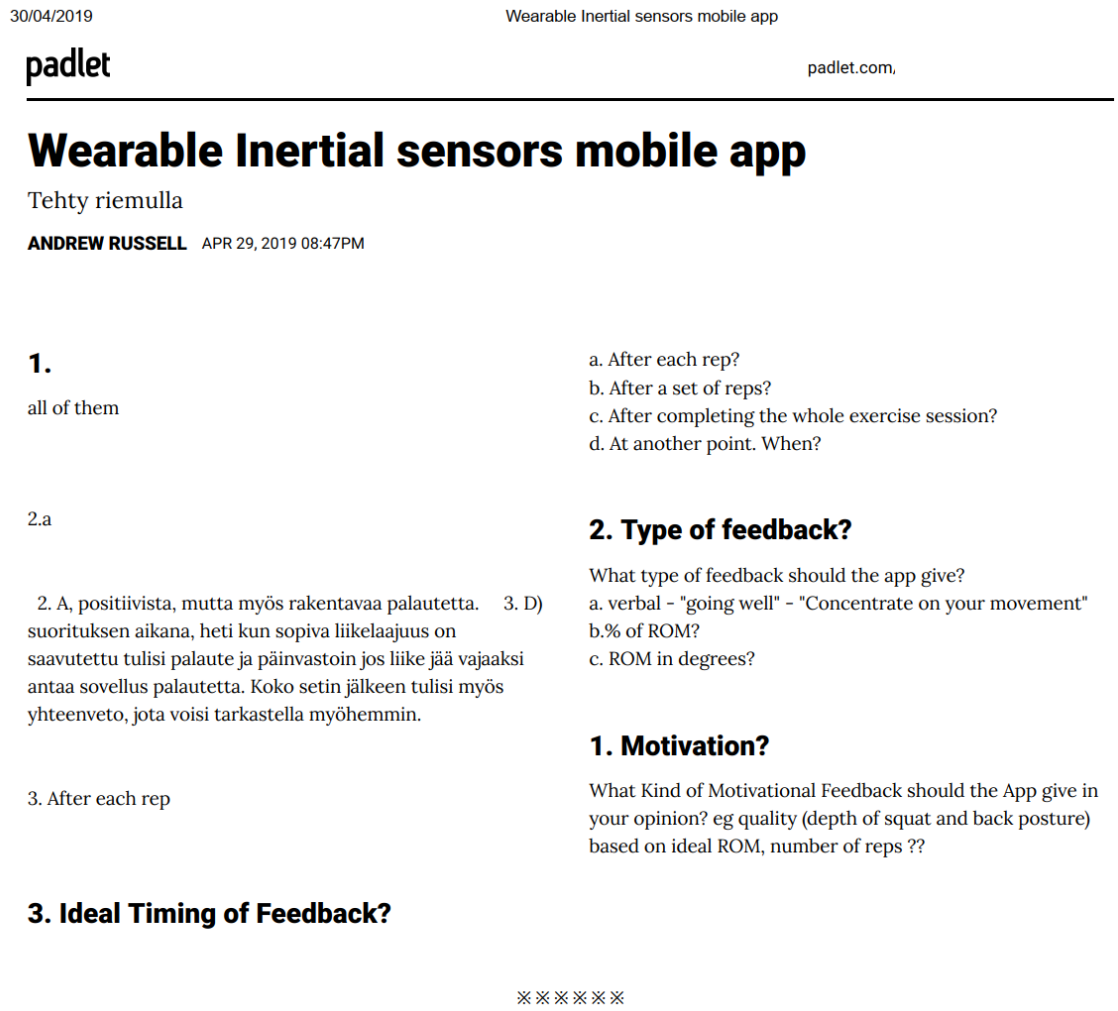

30/04/2019 Wearable Inertial sensors mobile app

padlet padlet.com,

Wearable Inertial sensors mobile app

Tehty riemulla

ANDREW RUSSELL APR 29, 2019 08:47PM

1.

all of them

2.a

2. A, positiivista, mutta myös rakentavaa palautetta. suorituksen aikana, heti kun sopiva liikelaajuus on saavutettu tulisi palaute ja päinvastoin jos liike jää vajaaksi antaa sovellus palautetta. Koko setin jälkeen tulisi myös yhteenveto, jota voisi tarkastella myöhemmin.

3. D)

3. After each rep

3. Ideal Timing of Feedback?

a. After each rep?
b. After a set of reps?
c. After completing the whole exercise session?
d. At another point. When?

2. Type of feedback?

What type of feedback should the app give?
a. verbal - "going well" - "Concentrate on your movement"
b.% of ROM?
c. ROM in degrees?

1. Motivation?

What Kind of Motivational Feedback should the App give in your opinion? eg quality (depth of squat and back posture) based on ideal ROM, number of reps ??

※※※※※※

Figure 36. First year students of physiotherapy group response to post presentation questions.

University of Applied Sciences first year physiotherapy students anonymous group feedback to post presentation questions. English translation to question 2 in Figure 35.

Positive but also constructive feedback. During the exercise regime as soon as the appropriate range of movement has been reached feedback should be given, and vice

versa if the range of movement is not reached, then the app should give feedback. After the whole set has been completed, there should also be a summary that could be viewed later.

Appendix B. Sampling method problems for FFT of angular acceleration

The first method used to calculate angular velocity and then angular acceleration, Backwards Difference Method (BDM) caused issues with the FFT transform. The method appears to have caused a phase shift which combined with the sampling frequency of 100Hz resulted in an amplitude spike at 24.7Hz. The trace is shown in Figure 33. The method was later changed for the main body of this study to the First Central Difference Method (FCDM) which did not cause a phase shift, and cause aliasing issues at 23.8Hz in the FFT.

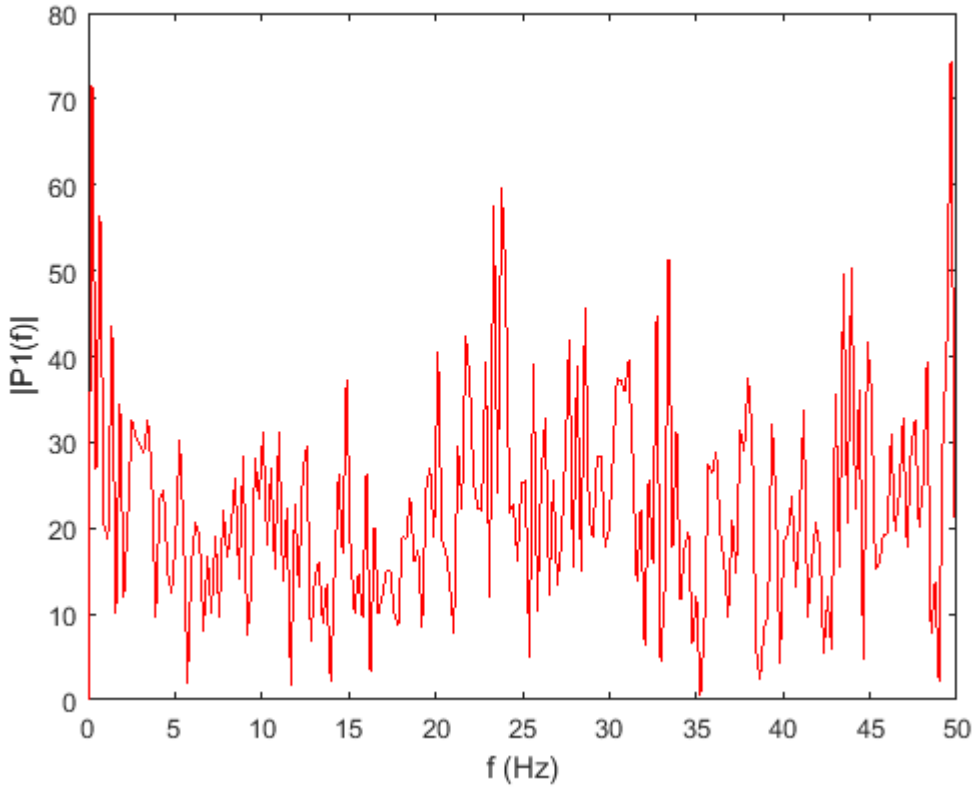

Figure 37. BDM method for thigh angular acceleration caused 23.7Hz aliasing in FFT.

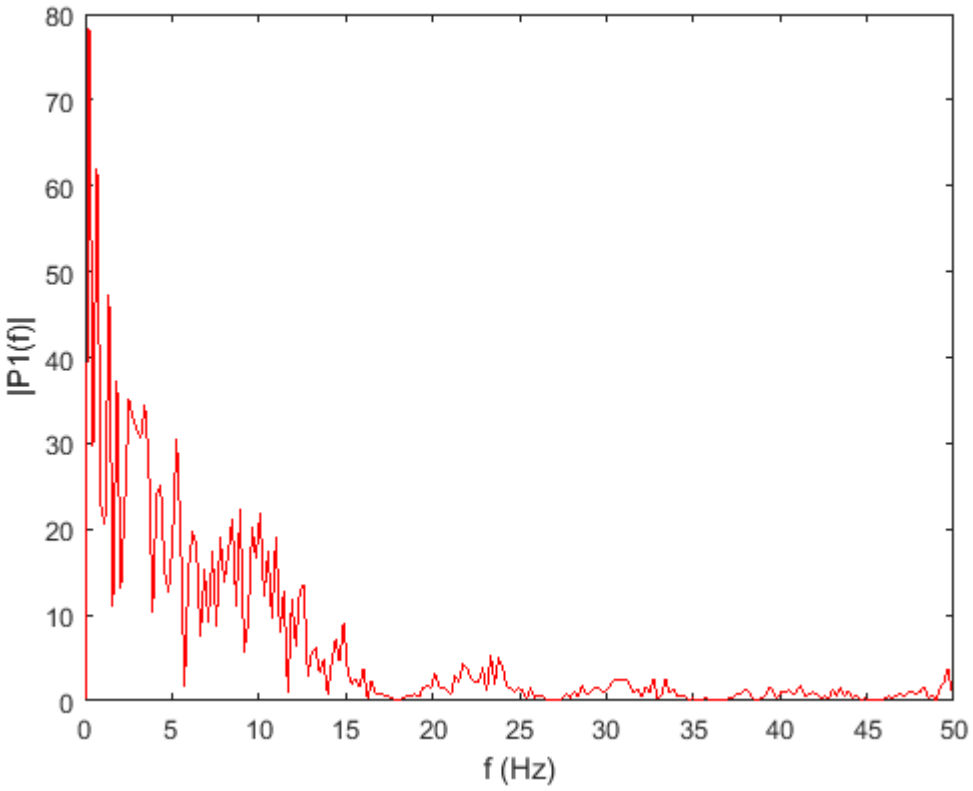

Figure 38. Low pass FIR 11Hz 10th order filter applied, removes 23.7Hz aliasing in FFT

Low pass Finite Impulse Response 11Hz filter applied to the FFT removes the aliasing at 23.7Hz (Figure 37).